Stars and Symbiosis: MicroRNA- and MicroRNA*-Mediated Transcript Cleavage Involved in Arbuscular Mycorrhizal Symbiosis[1][W][OA]

Emanuel A. Devers[2], Anja Branscheid[2], Patrick May[2,3,4], and Franziska Krajinski*

Max-Planck-Institute of Molecular Plant Physiology, 14476 Potsdam/Golm, Germany

The majority of plants are able to form the arbuscular mycorrhizal (AM) symbiosis in association with AM fungi. During symbiosis development, plant cells undergo a complex reprogramming resulting in profound morphological and physiological changes. MicroRNAs (miRNAs) are important components of the regulatory network of plant cells. To unravel the impact of miRNAs and miRNA-mediated mRNA cleavage on root cell reprogramming during AM symbiosis, we carried out high-throughput (Illumina) sequencing of small RNAs and degradome tags of *Medicago truncatula* roots. This led to the annotation of 243 novel miRNAs. An increased accumulation of several novel and conserved miRNAs in mycorrhizal roots suggest a role of these miRNAs during AM symbiosis. The degradome analysis led to the identification of 185 root transcripts as mature miRNA and also miRNA*-mediated mRNA cleavage targets. Several of the identified miRNA targets are known to be involved in root symbioses. In summary, the increased accumulation of specific miRNAs and the miRNA-mediated cleavage of symbiosis-relevant genes indicate that miRNAs are an important part of the regulatory network leading to symbiosis development.

Small silencing RNAs are a complex group of short RNAs with sizes in the range of approximately 20 to 25 nucleotides in length that can regulate gene expression at the transcriptional and posttranscriptional levels (Bartel, 2004; He and Hannon, 2004). In recent years, it has become evident that two main classes of small silencing RNAs, short interfering RNAs and microRNAs (miRNAs), are of great importance in plants. Small RNAs are involved in developmental processes, hormonal signaling, organ polarity, RNA metabolism, and abiotic and biotic stress responses (Rhoades et al., 2002; Borsani et al., 2005; Kidner and Martienssen, 2005; Nogueira et al., 2006; Laporte et al., 2007; Liu et al., 2007; Phillips et al., 2007; Sunkar et al., 2007; Willmann and Poethig, 2007; Zhou et al., 2007; Chen, 2008; Chinnusamy et al., 2008; Lu et al., 2008; Lu and Huang, 2008; Navarro et al., 2008; Zhao et al., 2009). Short interfering RNAs and miRNAs in plants are both generated by double-stranded RNA and have a similar size. Both groups of small RNAs have different origins, and they possess distinct biogenesis pathways (Carthew and Sontheimer, 2009; Ghildiyal and Zamore, 2009; Voinnet, 2009).

miRNAs in plants are mostly transcribed from intergenically located *MIR* genes through RNA polymerase II activity, resulting in a 5′ capped and 3′ poly (A) tailed primary transcript (Cai et al., 2004; Lee et al., 2004). A region within the primary transcript folds into an imperfect stem-loop structure, which is cut by Dicer-like (DCL) protein, resulting in a miRNA precursor. This precursor is subsequently processed by the same DCL protein to yield the miRNA/miRNA* duplex with a two-nucleotide overhang at the 3′ ends (Papp et al., 2003; Vazquez et al., 2004; Xie et al., 2004). In contrast to animal miRNAs, both duplex strands of plant miRNAs are 2′-*O*-methylated at their 3′ ends by HEN1 to prevent degradation (Yu et al., 2005; Yang et al., 2006). The duplex is then exported to the cytosol, presumably by HASTY (Park et al., 2005). An AGO protein then incorporates one of the duplex strands, which is then referred to as mature miRNA (Liu et al., 2004; Meister et al., 2004). Its counterpart from the duplex is called miRNA* and will often be degraded after release of the mature strand (Khvorova et al., 2003; Schwarz et al., 2003). The miRNA within the AGO protein then guides the RISC to the target mRNA (Bartel, 2009). This is achieved by pairing of the miRNA with a specific binding site within the target transcript (Wang et al., 2008a, 2008b). The RISC then suppresses expression of the transcript by inhibiting translation or transcript cleavage of the miRNA/target duplex, normally between the 10th and 11th nucleo-

[1] This work was supported by the Max-Planck Society.

[2] These authors contributed equally to the article.

[3] Present address: Luxembourg Centre for Systems Biomedicine, University of Luxembourg, 162a, Avenue de la Faïencerie, L–1511 Luxembourg, Luxembourg.

[4] Present address: Institute for Systems Biology, 401 Terry Ave. North, Seattle, WA 98109–5234.

* Corresponding author; e-mail krajinski@mpimp-golm.mpg.de.

The author responsible for distribution of materials integral to the findings presented in this article in accordance with the policy described in the Instructions for Authors (www.plantphysiol.org) is: Franziska Krajinski (krajinski@mpimp-golm.mpg.de).

[W] The online version of this article contains Web-only data.

[OA] Open Access articles can be viewed online without a subscription.

www.plantphysiol.org/cgi/doi/10.1104/pp.111.172627

tide positions from the miRNA 5′ end (Elbashir et al., 2001a, 2001b). In contrast to animals, where miRNAs often posttranscriptionally regulate gene expression via translational inhibition, it was estimated that plant miRNAs often lead to target cleavage due to a high degree of complementarity between target mRNA and miRNA (Rhoades et al., 2002). But it was demonstrated that both mechanisms are involved in plant miRNA function (Brodersen et al., 2008). miRNAs autoregulate their own biogenesis through targeting of *DCL1* and *AGO1* by miR162 and miR168 (Xie et al., 2003; Vaucheret et al., 2004).

The availability of deep sequencing technology had delivered a sharp rise in the number of identified miRNAs (Griffiths-Jones et al., 2008). However, without reliable target information, miRNA data sets are of limited biological value. Several computational methods of miRNA target prediction based on the perfect or near-perfect sequence complementary between a given miRNA and its target binding site are available. However, these in silico predictions often lead to a high false-positive rate (Jones-Rhoades and Bartel, 2004). Target cleavage by miRNAs can be identified via modified RNA ligase-mediated RACE, which uses the 5′-phosphate at the cleavage site derived from the AGO-mediated endonucleolytic cleavage (Elbashir et al., 2001b; Martinez et al., 2002). Deep sequencing of uncapped mRNA populations of a tissue combined with a bioinformatic analysis allows the transcriptome wide identification of miRNA-cleaved mRNAs (Addo-Quaye et al., 2008; German et al., 2008; Gregory et al., 2008).

There are now several lines of evidence that miRNAs play a significant role during the interaction of plants with symbiotic organisms. Recently, we demonstrated that mature miR399 is accumulating in roots of *Medicago truncatula* and tobacco (*Nicotiana tabacum*) plants during arbuscular mycorrhizal (AM) symbiosis (Branscheid et al., 2010). miRNAs are also known to be key players in the response to parasitic organisms. For instance, flagellin, which is a major pathogen-associated molecular pattern of *Pseudomonas syringae*, enhances the transcription of miR393, which targets the transcript of the F-box auxin receptor transporter response protein and a number of related proteins (Navarro et al., 2006; Fahlgren et al., 2007). General miRNA-defective Arabidopsis (*Arabidopsis thaliana*) mutants indicate an even more widespread role of miRNAs; these mutants are able to sustain disease from normally nonvirulent bacteria strains (Navarro et al., 2008). A successful development of tumors caused by *Agrobacterium tumefaciens* also requires an intact miRNA pathway, as Arabidopsis *dcl1* mutants are immune to crown gall formation (Dunoyer et al., 2006). Hence, there is increasing evidence that miRNAs are integral components of plant responses to adverse environmental conditions, including biotic interactions (Voinnet, 2008), in addition to their established functions during normal growth and development, such as hormone responses and meristem regulation (Kidner and Martienssen, 2005). Moreover, in *M. truncatula*, miR169 is important for the spatial and temporal restriction of the CCAAT-binding family transcription factor *MtHAP2-1* during symbiotic nodule development (Combier et al., 2006). miR166 is expressed in developing root and nodule tips, and overexpression in *M. truncatula* leads to a reduced number of lateral roots and symbiotic nodules (Boualem et al., 2008). A recent miRNA profiling in soybean (*Glycine max*) and *M. truncatula* led to the discovery of a number of new miRNAs regulated during nodule symbiosis (Subramanian et al., 2008).

AM symbiosis is formed by most flowering plants in association with glomeromycotian fungi. The establishment of an AM symbiosis requires an ongoing molecular dialogue between AM fungus and host plants, leading to the reprogramming of plant root cells for endosymbiosis (Kosuta et al., 2003, 2008; Akiyama et al., 2005). At later stages, the fungus forms the so-called arbuscules in cortical cells. The arbuscules are supposed to be the place of nutrient transfer from fungus to plant. Arbuscule-containing cells are the result of a complex reprogramming of noncolonized cortical cells. They show fundamental morphological and physiological changes. The fungal hyphae, which form tree-like hyphal branches inside the cortical cells, are surrounded by a novel membrane type, the periarbuscular membrane. The periarbuscular membrane can be regarded as an extension of the plasma membrane, but it shows striking changes in the composition of proteins (Pumplin and Harrison, 2009), especially with regard to transporter proteins (Javot et al., 2007; Benedito et al., 2010). In recent years, several studies analyzed transcriptome changes in plant roots after colonization by AM fungi (Liu et al., 2003; Wulf et al., 2003; Frenzel et al., 2005; Hohnjec et al., 2005; Fiorilli et al., 2009; Gomez and Harrison, 2009), demonstrating a massive reprogramming in response to AM colonization in the host cells, yet there is little information available about how these changes in gene expression are mediated (Krajinski and Frenzel, 2007).

In this work, we used deep sequencing, prediction, and read count-based expression profiling of miRNAs, which revealed novel and already annotated miRNAs with increased expression in mycorrhizal roots. In parallel, we carried out a degradome sequencing, which led to the identification of miRNA targets. Of these novel targets, several are already known to be involved in root symbiosis.

RESULTS

Deep Sequencing of *M. truncatula* Small RNAs and Degradome Tags

The goal of this study is to identify miRNAs and miRNA targets that are related to transcriptional reprogramming of plant cells during AM symbiosis. For

this purpose, we used high-throughput sequencing with Illumina technology to detect and profile miRNAs and miRNA targets of *M. truncatula*. We inoculated *M. truncatula* seedlings with *Glomus intraradices*, harvested the mycorrhizal plants and noninoculated nonmycorrhizal plants at 3 weeks after inoculation, and extracted root RNA. Two small RNA (sr) and degradome (deg) libraries were prepared from either mycorrhizal (myc) or nonmycorrhizal (nm) roots of *M. truncatula*. In total, we obtained more than 30 million reads (Table I), and more than 97% of all reads were of the appropriate sizes (i.e. 15–31 nucleotides for the small RNA libraries and 20–21 nucleotides for the degradome libraries). Within the small RNA libraries, the 21- and 24-nucleotide molecules were the most abundant forms, and the 24-nucleotide small RNAs were more diverse than the 21-nucleotide class (Fig. 1). Within the degradome libraries, we obtained slightly more 20- than 21-nucleotide sequences (Fig. 1).

Mapping of Small RNAs and Degradome Tags to the *M. truncatula* Genome

The small RNA reads from both libraries were 3′ trimmed, and reads containing low-complexity regions [e.g. poly(A) stretches] and low-quality reads (containing N's) were removed. Reads were filtered for length between 15 and 31 nucleotides. The reads of both libraries (sr-myc and sr-nm) were mapped to the *M. truncatula* genome (versions 2.0 and 3.0), annotated cDNA sequences, annotated noncoding RNA, and available *G. intraradices* sequences (The Glomus Consortium, unpublished data) using 100% (no mismatch) as an identity threshold. Sixty-nine percent of redundant sr-myc and 72% of sr-nm could be mapped with 100% identity to the *M. truncatula* genome. Of the sr-myc reads, 1.6% could be mapped with 100% identity to *G. intraradices* sequences. Of the 0.05% reads of the nm libraries that match *G. intraradices* sequences, 95% are rRNA sequences. Thirty-nine percent and 38% of nonredundant nm and myc reads, respectively, were assigned to uncharacterized regions of the mt3.0 genome, supporting the assumption that most small RNAs originate from intergenic regions. A summary of the read annotation of redundant (total) and nonredundant (unique) sr reads is shown in Figure 2.

Mapping the degradome tags with 100% identity to *M. truncatula* and *G. intraradices* sequences revealed matches of 86% and 76% of total nm-deg and myc-deg sequences to the mt3.0 genome, respectively. Of the myc-deg sequences, 7.7% mapped to *G. intraradices* sequences. The higher proportion of degradome tags mapping to *G. intraradices* as compared with the small RNAs is due to the fact that most degradome tags are of mRNA origin and available *G. intraradices* sequences contain a high proportion of mRNA sequencing data (The Glomus Consortium, unpublished data). A summary of the read annotation of redundant and nonredundant degradome reads is shown in Figure 3.

The Degradome Sequences Are Correlated to Transcriptome Data of Mycorrhizal and Nonmycorrhizal Roots

Recent degradome analyses in rice (*Oryza sativa*) and Arabidopsis showed that only a small fraction of these sequence tags represent miRNA-mediated transcript cleavage (Li et al., 2010; Zhou et al., 2010b); the vast majority of these sequence tags represent non-miRNA-mediated, unspecific RNA degradation. This means that degradome sequence tag data of two tissues can be used to compare expression levels when neglecting the proportion of miRNA-mediated mRNA cleavage in the data set. Hence, a correlation of transcript abundance represented by read counts for each transcript between both tissues in the degradome libraries and previous transcriptome studies is expected. We analyzed transcript regulation by calculating read counts in both degradome libraries and compared the $\log_2$ fold changes with transcriptome data obtained by microarray hybridization of mycorrhizal versus nonmycorrhizal *M. truncatula* roots (Gomez et al., 2009). To compensate ratio compression by saturation effects on microarrays, strongly specifically expressed genes (no sequence tags in one condition and at least 10 tags in the second condition), we used the half minimum normalized abundance for those transcripts. The comparison between $\log_2$ fold change values of both data sets revealed a significant correlation (Pearson correlation coefficient = 0.51, $P < 0.00001$; Supplemental Fig. S1). Hence, the degradome sequencing data can be used to detect

Table I. *Statistics of the Illumina sequencing of two small RNA (sr) and two degradome (deg) libraries*

There were 15 to 31 nucleotides for small RNA sequence tags and 20 to 21 nucleotides for degradome sequence tags. myc, Mycorrhizal roots; nm, nonmycorrhizal roots.

Read Data	sr-nm	sr-myc	deg-nm	deg-myc
Raw reads	8,620,161	8,359,230	5,737,931	7,907,566
Reads of appropriate size	8,350,029	8,187,981	5,620,484	7,777,769
Unique reads of appropriate size	3,798,457	3,878,418	2,897,498	4,594,450
Percentage of total reads mapping to *M. truncatula* mt3.0 (100% identity)	72.28	69.14	85.86	75.77
Percentage of total reads mapping to *G. intraradices* (100% identity)	0.05	1.57	0.05	7.65

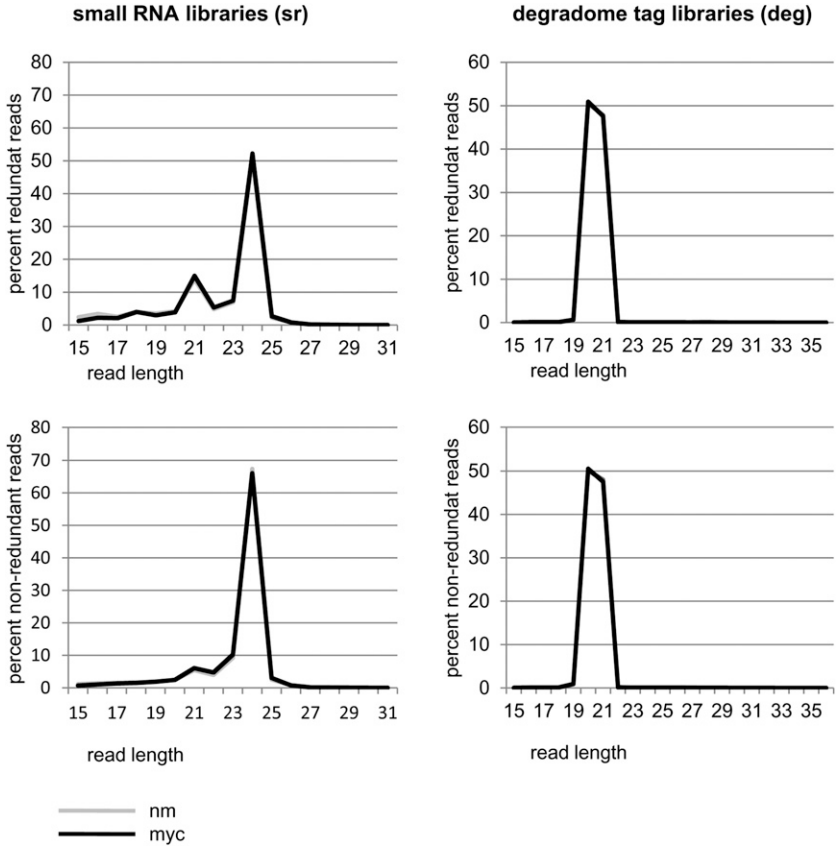

Figure 1. Read length distribution of the small RNA and degradome libraries.

miRNA-mediated mRNA cleavage; in parallel, they can also be used to investigate transcriptional changes between the two tissues.

Analysis of Annotated miRNAs

In order to investigate the expression of known (miRBase 16 annotated) miRNAs in mycorrhizal and nonmycorrhizal roots, we searched for known miRNAs in our small RNA libraries. A total of 375 *M. truncatula* miRNAs are currently annotated at the miRBase (release 16) database (Griffiths-Jones et al., 2008). A total of 162 mature miRNAs could be identified through 100% matches of reads to the mature sequence in one or both of our libraries (Supplemental Table S1), representing 43.2% of the currently known *M. truncatula* miRNAs. Next, we analyzed any reads matching the annotated miRNA* or precursor sequences. Surprisingly, in some cases, we found reads matching the miRBase-annotated precursor sequence, but reads matching the annotated mature miRNA sequences with 100% identity were absent. This indicates that some miRNAs can occur as different isoforms or siblings (Vazquez et al., 2008; Zhang et al., 2010; i.e. miRNAs originating from the same primary transcript with distinct mature forms). miRNA isoforms (isomiRs) often contain a small sequence shift or additional nucleotides (Ebhardt et al., 2010), whereas miRNA siblings are nonoverlapping in comparison with the originally annotated mature or star miRNAs (Zhang et al., 2010). We detected 17 isoforms of miRNAs whose mature sequence was missing (miR169e/h/i/n/o, miR393b, miR2594a/b, miR2611, miR2674, miR2678, miR2679c, and miR2680a-e). In addition, for two miRNAs, we found reads of the annotated star sequence but no reads matching the mature sequence (miR171f and miR398a). Taking this into account, we found a total of 181 known miRNAs in mycorrhizal and nonmycorrhizal *M. truncatula* roots.

To investigate the specific abundance of annotated mature miRNAs and the corresponding miRNA* and found isomiRs, we calculated the read counts of the corresponding sequences in our small RNA libraries. Interestingly, for 11 miRNAs, the isoforms of the mature strand were found to have a higher abundance than the sequence annotated as mature miRNA sequence at miRBase (miR156, miR166b/c/f, miR1509a, miR1519b, miR2597, miR2610a/b, miR2620, and miR2645). In addition, we found a high abundance for miRNA* sequences of several legume-specific miRNAs like miR1507*, miR2086*, miR2089*, and miR2118* (Szittya et al., 2008; Jagadeeswaran et al., 2009). Additionally, the star strand for eight miRNAs (miR160b/e, miR169d/l/m, miR369a, miR2089, and miR2118) and a different isoform of 19 miRNA star strands (miR171c, miR2088a, miR2592a–g/i-j/o–s, miR2595, and miR2612a/b) showed a higher abundance than the corresponding mature strand. Four miRNAs showed a similar expres-

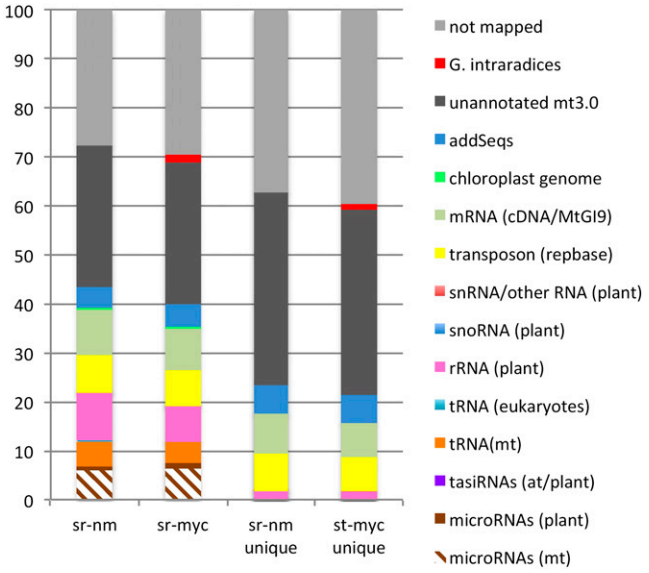

Figure 2. Summary of annotation results of the small RNA libraries. Small RNA sequences were mapped to relevant functional classes, which are distinct from bottom to top. addSeqs, Additional mt3.0 (Illumina) sequences.

sion of the mature and star strands (miR172 and miR399c/j/k). Hence, we could identify 48% of all annotated *M. truncatula* miRNAs in our two small RNA libraries. Notably, a high proportion of these miRNAs seemed to occur in different isoforms than the annotated mature miRNA sequence.

Prediction of Novel *M. truncatula* miRNAs

In order to find novel *M. truncatula* miRNAs, we subjected the 15- to 31-nucleotide reads of the small RNA libraries to a miRNA prediction pipeline. In order to calculate the discovery rate of the adapted miRDeep algorithm, we analyzed the ability of the algorithm to recover previously annotated miRNAs from a given data set. To simulate the prediction pipeline as described in "Materials and Methods," where we excluded reads that matched known miRNAs, we used for evaluation only reads that were sequenced at least 20 times, that were not matching more than 25 times on the *M. truncatula* genome mt3.0, and that matched with 100% in the sense direction onto annotated miRNA precursor sequences.

Only 139 of the 340 nonredundant miRBase precursors had at least one read with an abundance greater than 20, which is the minimum threshold we used for prediction before. Only 96 of these 139 known miRNA precursors had a mature miRNA read abundance of at least 20 reads. Since the excising of the correct precursor sequence depends on the position and hybridization of the (most likely) mature miRNA, we assume here that using the described parameters, the new method should be able to predict those 96 known miRNAs from the given data set. Using exactly the same prediction pipeline as for the new miRNAs (see "Materials and Methods"), we could predict 87 (90.26%) of the known miRNAs (data not shown). Applying the plant miRDeep program to our small RNA data sets revealed the prediction of 515 novel miRNA candidates of 20- to 25-nucleotide length.

To further validate these 515 miRNA candidates, we included criteria for plant miRNA annotation (Meyers et al., 2008). All 515 predicted miRNA candidates are produced from a single-stranded stem-loop precursor, which is required for miRNA prediction within the miRDeep pipeline. For 69 candidate miRNAs, the corresponding miRNA* sequence was present in the deep sequencing data; hence, these candidates fulfill the primary criterion for miRNA annotation. An additional 369 out of 515 miRNA candidates satisfy at least one of the ancillary criteria, including conservation among one or more plant species, clustering into miRNA families, and confirmed target by degradome analysis. However, criteria for miRNA annotation from deep sequencing data have been updated recently and now include the requirement that high-confidence miRNAs have multiple cloned nucleotide reads with relatively fixed 5′ ends at both arms of the precursor sequence and the possibility to identify the miRNA/miRNA* duplex pair (Berezikov et al., 2010). Taking these criteria into account, we annotated 243 of our miRNA candidates as miRNAs at miRBase (Griffiths-Jones et al., 2008). A list of these miRNAs is shown in Supplemental Table S2; the remaining 272 miRNA candidates from the miRDeep prediction are

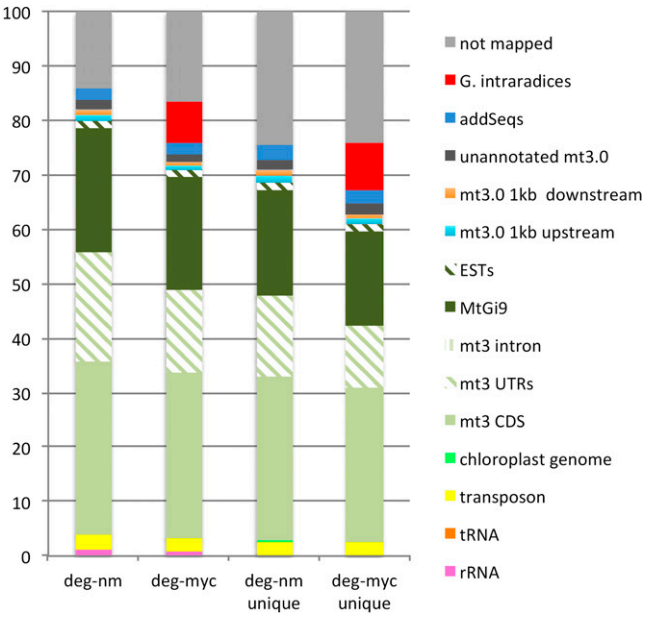

Figure 3. Summary of annotation results of the degradome libraries. Degradome sequence tag sequences were mapped to relevant functional classes, which are distinct from bottom to top. addSeqs, Additional mt3.0 (Illumina) sequences.

listed in Supplemental Table S3. Of the novel 243 miRNAs deposited at miRBase, 74 are novel conserved miRNAs and 169 miRNAs belong to 95 novel plant miRNA families. Of the 169 novel miRNAs, 74 showed homologous sequences (less than three mismatches) in one the following organisms: Arabidopsis, maize (*Zea mays*), *Lotus japonicus*, soybean, or *Populus trichocarpa*, indicating that 44% of novel miRNAs are also conserved within other plants. Data of novel miRNAs and miRDeep-predicted candidate miRNAs are deposited at http://mirmyc.mpimp-golm.mpg.de and will be updated to novel *M. truncatula* genome versions if available.

Expression Profiling of miRNAs by Read Count Analysis

In order to investigate a putative role of novel and conserved miRNAs in the mycorrhizal symbiosis, we searched for miRNAs with induced or decreased expression in mycorrhizal roots when compared with nonmycorrhizal roots. To identify these differentially expressed miRNAs, the abundances of miRNAs were calculated by comparing the normalized numbers of reads in both libraries. Using a $\log_2$ fold cutoff of 0.7, 20 distinct miRNA sequences showed a differential abundance between mycorrhizal and nonmycorrhizal roots (Table II). miR5229a/b showed the strongest elevated abundance levels ($\log_2$ fold change of 9.7) in mycorrhizal roots as compared with nonmycorrhizal roots. Interestingly, we also found miRNA* sequences to be regulated in mycorrhizal roots. miR169d*/l*/m*/e.2* was more abundant as the annotated mature miRNA sequence and, in addition, 4-fold more abundant in mycorrhizal roots. This is of particular interest because the miR169d*/l*/m*/e.2* target identified by degradome analyses (see below) is *MtBcp1*, which itself is specifically transcribed in arbuscule-containing cells. In addition, miR160f* was not detected in nonmycorrhizal roots but was clearly abundant in mycorrhizal roots. In summary, we could identify 20 miRNAs with significantly (χ^2 test, $P \leq 0.05$) changed expression in mycorrhizal roots, indicating a role for these miRNAs in mycorrhizal symbiosis.

Identification of miRNA Cleavage Targets by Degradome Analysis

The small RNA sequences presented here revealed the identification of 243 novel miRNAs and additional miRNA candidates. However, these data offer limited biological information without reliable target identifications in order to get information about the cellular processes where these miRNAs might be involved. For this purpose, we carried out a degradome analysis, which is a large-scale experimental method for miRNA target identification. Sequencing degradome libraries of *Medicago* nonmycorrhizal and mycorrhizal roots revealed a total of 5.6 million and 7.8 million reads, respectively. In order to find miRNA cleavage sites in the *M. truncatula* root transcriptome, we subjected the 20- and 21-nucleotide distinct reads to the CleaveLand pipeline (Addo-Quaye et al., 2009) version 2.0. We were able to identify 371 and 404 cleavage sites for miRBase-annotated miRNAs within the *M. truncatula* genome sequence and the *Medicago truncatula* Gene Index (MtGI) cDNA sequences, respectively (Supplemental Table S4). After searching for targets for the 243 novel miRBase-annotated miRNAs of this study, we found 56 cleavage sites in mt3.0 sequences and 62 cleavage sites in MtGI sequences (Supplemental Table S). Surprisingly, the degradome analysis showed 44 targets of both databases that are cleaved by miRNA* (Table III). In total, we identified 185 mRNAs (mt3.0) to be miRNA, miRNA*, or miRNA candidate cleavage targets, of which 157 are targets of the novel miRBase-annotated miRNAs. We next wanted to estimate the frequency of miRNA-mediated mRNA cleavage in the *M. truncatula* root transcriptome. The degradome sequence tags could be mapped to 27,729 mt3.0 genes. Hence, we detected miRNA-mediated transcript cleavage for 0.67% of the represented root transcriptome. For a functional characterization of all miRNA targets identified, we carried out a MapMan analysis (Usadel et al., 2005). Interestingly, disease resistance proteins (27 genes) and transcription factors (33 genes) were clearly overrepresented within the identified target genes (Fig. 4). This indicates that particularly the transcript regulation and the defense responses are controlled by miRNA-mediated mRNA cleavage in roots.

miRNA- and miRNA*-Mediated mRNA Cleavage Events Were Found for Genes Involved in Root Endosymbioses

We wanted to investigate if transcripts that are highly regulated in mycorrhizal roots also represent miRNA targets. For this purpose, we used a read count analysis of our degradome sequence tags to identify transcripts that are strongly overrepresented or underrepresented in mycorrhizal roots as compared with nonmycorrhizal roots. The $\log_2$ fold values were calculated for each of the 27,729 genes detected in the degradome sequences. Using a $\log_2$ fold cutoff of ± 1, we could identify 111 miRNA targets with differential transcription in mycorrhizal versus nonmycorrhizal roots. Table IV shows all detected miRNA targets with a $\log_2$ fold cutoff of ± 1.5. The most strongly regulated miRNA target (Medtr8g109760.1) encodes a putative GRAS transcription factor, which is specifically transcribed in arbuscule-containing cells (N. Gaude, S. Bortfeld, N. Duensing, M. Lohse, and F. Krajinski, unpublished data). Interestingly, transcripts encoding a putative phosphate transporter (Medtr5g076920.1) strongly accumulate in mycorrhizal roots and are a target of the miR399 family. In addition, we identified previously described mycorrhizal symbiosis-induced genes to be miRNA targets, such as *MtBcp1* (Medtr7g102930.1; Pumplin and Harrison, 2009; Parádi et al., 2010), which is cleaved by miR169d*/l*/m*/e.2* (Fig. 5E). Additionally, this miRNA itself is induced in

Table II. Differentially expressed miRNAs and their confirmed and predicted targets

A complete list of miRNAs and their corresponding targets including target accession numbers can be found in Supplemental Table S7.

miRNA Identifier	Sequence	Length	rpm[a] myc	rpm[a] nm	LFC[b]	Target Gene Family
miR5229a,b	TTAGCAGGAAGAGTGACTATG	21	98.9	0	9.7	Heme peroxidase[c] HSP20-like chaperone[c]
miR5206	ATGGGATCCTGTTGGTGGGTTAC	23	3.7	0.1	4.9	Hypothetical protein[d]
miR160f*	GCGTGAAGGGAGTCAAGCAGG	21	3.4	0	4.8	Hypothetical protein[c] Putative periplasmic lipoprotein[c]
miR5204	GCTGGAAGGTTTTGTAGGAAC	21	36.3	1.7	4.4	Heavy metal transport protein[c] Zinc finger transcription factor[c] Nucleotide-binding protein[c] RNA-binding protein[c] Protein kinase-like protein[c]
miR169d, l	AAGCCAAGGATGACTTGCCGG	21	6.4	0.4	4.1	CCAAT transcription factor[c,d] Hypothetical protein[c,d] MMS sensitivity-related protein[c,d]
miR169d*,e.2*,l*,m*	GGCAGGTCATCCTTCGGCTATA	22	20.9	1.3	4	Blue copper-binding protein[d] Glycoside hydrolase[c] Ser/Thr protein kinase[c]
miR160c	TGCCTGGCTCCCTGAATGCCA	21	14.4	2.8	2.4	Auxin response factor[c,d] Hypothetical protein[d]
miR171h	CGAGCCGAATCAATATCACTC	21	345.6	153.9	1.1	Pentatricopeptide repeat protein[c,d] GRAS transcription factor[c,d] Nodulation-signaling pathway 2 protein[c,d] E2 ubiquitin-conjugating enzyme[c] Plant lipid transfer protein[c] Protein kinase[c]
miR167	TGAAGCTGCCAGCATGATCTA	21	869.5	401	1.1	Auxin response factor[d] WD40-like protein[d] Zinc finger transcription factor[c] Sodium/hydrogen exchanger[c] Protein kinase[c]
miR5244	TATCTCATGAAGATTGTTGGT	21	22.8	11.1	1	Leu-rich repeat protein[c]
miR5232	TACATGTCGCTCTCACCTGAA	21	110.2	54.7	1	Glycoside hydrolase[d] Type IIB calcium ATPase[c,d] Protein kinase[c]
miR5281b–f	TCTTATAAATAGGACCGGAGGGAG	24	28.58	14.73	0.9	Alcohol dehydrogenase superfamily[c] TIR; disease resistance protein[c] COG complex component[c] H^+-transporting two-sector ATPase[c] Zinc finger transcription factor[c] Putative Fru-1,6-bisphosphatase[c] Cyclin-like F-box protein[c] Nodule-specific Cys-rich peptide[c]
miR5250	TGAGAATGTTAGATACGGAAC	21	223	123.1	0.8	ATP-binding protein[d] Glycosyl transferase[c]
miR2086	GACATGAATGCAGAACTGGAA	21	2,167.9	1,204	0.8	Biotin-binding site protein[d] Argonaute and Dicer proteins[c] Antihemostatic protein[c]
miR166b.2,c.2,f.2	TCTCGGACCAGGCTTCATTCC	21	5,653.9	3,158.8	0.8	HD-Zip transcription factor[c,d] Sugar transporter superfamily[c]
miR396b*	GTTCAATAAAGCTGTGGGAAG	21	124.08	73.64	0.8	FAD/NAD(P)-binding protein[c] Pentatricopeptide repeat protein[c] Leu-rich repeat protein[c] DNA methylase[c]
miR5213	TACGTGTGTCTTCACCTCTGAA	22	1,038.96	625.99	0.7	TIR; disease resistance protein[c,d]
miR162	TCGATAAACCTCTGCATCCAG	21	59.72	36.05	0.7001	Argonaute and Dicer proteins[c,d] FAD/NAD(P)-binding protein[c] Pentatricopeptide repeat protein[c] RNase[c]
miR4414a	AGCTGCTGACTCGTTGGTTCA	21	124.69	206.23	−0.8	Nuclear protein SET[c]

(*Table continues on following page.*)

Table II. (*Continued from previous page.*)

miRNA Identifier	Sequence	Length	rpm[a] myc	rpm[a] nm	LFC[b]	Target Gene Family
miR5285a–c	TGGGACTTTGGGTAGAATTAGGCG	24	12.09	25.03	−1.1	Zinc finger transcription factor[c] Sulfotransferase[c] Histone-like protein[c] XYPPX repeat protein[c] TIR; disease resistance protein[c] Proteinase inhibitor[c] β-Lactamase-like[c] Reverse transcriptase-like protein[c] Methyltransferase[c] Bacteriophytochrome[c] Proteasome subunit[c] GTP-binding protein[c]

[a]rpm, Reads per million. [b]LFC, $\log_2$ fold change ($P \leq 0.05$; χ^2 test together with Benjamini-Hochberg P value correction). [c]psRNATarget-predicted target (http://bioinfo3.noble.org/psRNATarget/), expectation range ≤ 3. [d]Target cleavage confirmed experimentally by degradome analysis.

mycorrhizal roots (Table II). Interestingly, we found that one mycorrhizal symbiosis-specific transcript, *MtGst1* (Wulf et al., 2003), seems to be a target of miR5282 and in addition of the predicted miRNA candidate new_miRc_275 (Fig. 5B). It is further worth mentioning that *MtNsp2* transcripts, which are a target miR171h (Fig. 5A), show elevated levels ($\log_2$ fold of 1.6) in mycorrhizal roots. Figure 5 shows additional target plots indicating the mRNA cleavage mediated by miRNAs induced in mycorrhizal roots, namely miR160c and miR167, both cleaving mRNAs encoding auxin response factors (Fig. 5, C and D), and miR169, targeting a CCAAT-binding transcription factor in mycorrhizal roots (Fig. 5F). Notably, within the population of transcripts with decreased levels in mycorrhizal roots, disease resistance genes are highly overrepresented. We found 16 miRNA cleavage sites within disease resistance genes encoding transcripts with decreased levels in mycorrhizal roots.

Quantitative PCR Expression Analysis

To confirm the regulation of selected miRNAs, we carried out quantitative real-time (qRT)-PCR analysis. In addition to mycorrhizal roots, we measured mature miRNA abundance in nodulated roots fertilized with either 20 μM or 1 mM phosphate and in roots grown under full nutrition (1 mM phosphate and 5 mM nitrate). This allows, to our knowledge, a first insight into the specificity of miRNA regulation with regard to nodule symbiosis and nutrient availability. The mature miRNA abundance was measured by stem-loop qRT-PCR (Chen et al., 2005; Fig. 6).

For expression analysis, we selected miR5229a/b and miR5204 because of their strongly elevated levels in mycorrhizal roots. In addition, miR160f* was chosen for expression analysis because this miRNA was undetectable in nonmycorrhizal roots. Also, miR160c was selected due to the elevated levels of mature miRNAs in mycorrhizal roots and additionally because it belongs to the same family as the mycorrhizal root-specific new miR160f*. As expected, qRT-PCR confirmed the induction in mycorrhizal roots as compared with nonmycorrhizal roots. Two of the measured miRNA candidates (miR160f* and miR5229a/b) were only detectable in mycorrhizal roots. miR160c showed an increased abundance in mycorrhizal roots as compared with all other treatments measured. miR167 was induced in mycorrhizal roots as compared with nonmycorrhizal roots under low phosphate but showed increased expression in nodulated roots and under full nutrition. miR169 and miR169d*/e.2*/l*/m* showed clear positive responses to increased phosphate nutrition. miR171h exhibited strongest expression in nodulated roots. This is of particular interest since we identified *MtNsp2*, a transcription factor necessary for nodulation symbiosis signaling (Kaló et al., 2005), to be a target of this miRNA (Table III; Supplemental Table S4). miR5204 was increased in mycorrhizal roots according to the read count analysis, which could be confirmed by qRT-PCR. However, we found further increased expression under full nutrition, indicating phosphate to be a positive regulator of miR5204. Comparable low expression levels of this miRNA in nodulated roots grown at high phosphate might be due to the root nodules as strong phosphate sinks. In summary, the expression profiling showed miRNAs specifically accumulating in mycorrhizal roots as well as miRNAs induced in mycorrhizal roots but also regulated by other stimuli.

Localization of Mature and Star miRNAs by in Situ Hybridization

Mature miRNAs and star sequences that were proven to show elevated levels in mycorrhizal roots were analyzed by in situ hybridization in order to get information about their spatial accumulation in mycorrhizal roots. As a negative control, we used a digoxigenin-labeled scramble probe, which is a ran-

Table III. *miRNA*-mediated mRNA cleavage detected by degradome analysis identified by CleaveLand 2.0 (Addo-Quaye et al., 2009)*
Listed accession numbers of the mt3.0 and MtGI databases are nonredundant.

miRBase Identifier	Cleavage Site	Alignment Score	Category nm	Category myc	Accession No.	Target Gene Family
MIR5204*	765	1.5	No tag	2	Medtr8g109760.1	GRAS transcription factor
MIR5204*	72	2.5	No tag	4	TC139113	TC139113
MIR5211*	290	3	No tag	4	CB892526	Hypothetical protein
miR172b*	511	6.5	2	2	Medtr7g040960.1	Albumin I
miR172b*	1,008	1.5	No tag	3	Medtr4g132640.1	*S*-Adenosyl-L-homocysteine hydrolase
MIR156b*	3,663	5.5	1	2	Medtr4g156260.2	Armadillo-like helical protein
MIR156i*	102	4.5	No tag	1	Medtr2g038500.1	Hypothetical protein
MIR160*	1,648	3.5	4	No tag	Medtr4g130250.1	Poly(A)-binding protein
MIR166e*	834	5.5	No tag	3	Medtr8g133160.3	Suc synthase
MIR166h*	1,883	3.5	4	2	Medtr8g016500.1	Tyr protein kinase
MIR166h*	571	3.5	2	No tag	Medtr8g140110.1	Protein phosphatase 2C
MIR169d*,e.2*,l*, m*	496	5.5	No tag	3	Medtr7g102930.1	Blue (type 1) copper domain
MIR172*	3,369	6	2	1	Medtr5g093930.1	Peptidase C19
MIR172*	532	6	0	2	Medtr3g020380.2	Annexin
MIR398a*	1,222	6	2	0	Medtr3g102850.1	Short-chain dehydrogenase
MIR398a*	840	6	1	2	TC114776	Deaminase
MIR398a*	458	6	1	No tag	TC137315	Hypothetical protein
MIR399c*, k*	356	2	4	No tag	Medtr4g135140.1	Hypothetical protein
MIR399c*, k*	134	2	4	No tag	Medtr4g135420.1	Hypothetical protein
MIR399d*	572	6.5	1	0	AC225519_18.2	α-Helical ferredoxin
MIR399k*	122	6	No tag	1	AW693165	TIR; disease resistance
MIR399h*	808	6	1	4	Medtr1g121460.2	CD9/CD37/CD63 antigen
MIR399h*	196	5.5	0	No tag	Medtr7g026570.1	Protein kinase
MIR399q*	972	6.5	1	2	Medtr3g080760.1	Nucleotide-binding protein
MIR399q*	665	6	1	4	TC138105	Protein kinase family
miR1510a*	678	4	3	No tag	Medtr4g114680.1	TIR; disease resistance
miR1510a*	727	4	3	No tag	Medtr6g098900.1	TIR; disease resistance
miR1510a*	8,901	4	3	No tag	Medtr6g099020.1	TIR; disease resistance
miR1510a*	741	4	3	No tag	Medtr6g099070.1	TIR; disease resistance
miR1510a*	8,902	4	3	No tag	Medtr6g099090.1	TIR; disease resistance
miR1510a*	699	4	3	No tag	Medtr6g099150.1	TIR; disease resistance
miR1510a*	685	4	3	No tag	Medtr6g099160.1	TIR; disease resistance
miR1510b*	284	7	0	2	BE240495	PR10-1 protein
miR1510b*	392	7	0	2	BF649495	PR10-1 protein
miR1510b*	2,942	7	2	2	DY615507	PR10-1 protein
miR1510b*	452	7	2	2	TC118500	PR10-1 protein
miR1510b*	519	7	2	2	TC118796	PR10-1 protein
miR1510b*	491	7	2	2	TC118868	PR10-1 protein
miR1510b*	491	7	0	2	TC121811	PR10-1 protein
miR1510b*	567	7	2	2	TC125034	PR10-1 protein
miR1510b*	237	7	2	2	TC128485	PR10-1 protein
miR1510b*	418	7	2	2	TC131880	PR10-1 protein
miR1510b*	244	7	0	2	TC132039	PR10-1 protein
miR1510b*	633	7	2	2	TC141258	Pro-rich cell wall protein

dom 21-nucleotide locked nucleic acid-enhanced DNA oligonucleotide (5′-GTGTAACACGTCTATACGCCCA-3′) not similar to any known plant transcript. Specific signals were observed for each of the six locked nucleic acid probes (Fig. 7), whereas no signals were observed after hybridization to a scramble probe.

Mature miR5229a/b strongly accumulated in arbuscule-containing cells in the root cortex. However, the signal strength varied between distinct arbuscule-containing cells, indicating that miR5229a/b is involved in specific stages of arbuscule development. The second mycorrhizal root-specific miRNA, miR160f*, strongly accumulated in the phloem and also in arbuscule-containing cells in the cortex. A similar accumulation pattern was observed for miR160c, supporting the fact that both molecules belong to the same miRNA family. miR5204, which was also regulated by phosphate, accumulated in arbuscule-containing cells and also strongly around fungal hyphae. Interestingly, not all arbuscule-containing cells showed accumulation of miR5204. The miR169d*/l*/m*/e.2* probes revealed no signals in arbuscule-containing cells but seemed to accumulate around intercellular fungal hyphae. The miR169 probe revealed a similar accumulation pattern. Strong hybridization signals were detected in the phloem and in addition around fungal hyphae in the intercellular space.

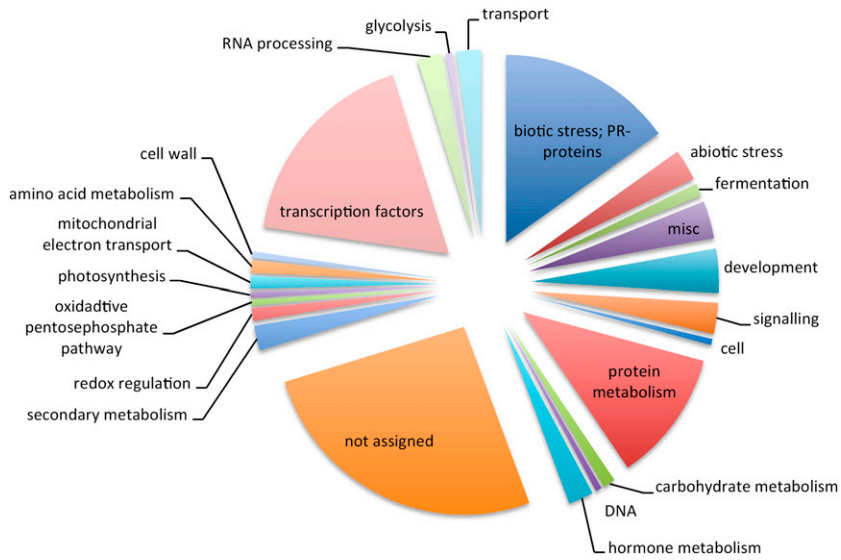

Figure 4. MapMan annotation of miRNA targets (mt3.0).

DISCUSSION

The aim of this work was to identify miRNAs and miRNA targets related to AM symbiosis in *M. truncatula* roots. The genome-wide profiling carried out in this study revealed the identification of more than 500 novel miRNA candidates. Of these candidates, 243 are now annotated at miRBase as novel *M. truncatula* miRNAs. The high number of miRNA candidates and annotated miRNAs expressed in *M. truncatula* roots indicates that miRNAs mediate a substantial part of the cellular regulation in plant roots. The biological value of such small RNA deep sequencing data sets is limiting, unless reliable data on miRNA targets are available. Current in silico miRNA target prediction tools in plants generally depend on complementary searches, based on perfect or nearly perfect base pairing between a mature miRNA and its target mRNA (Dai et al., 2011). The high-throughput sequencing of the degradome is one possibility for the experimental identification of miRNA-mediated transcript cleavage (Addo-Quaye et al., 2008; German et al., 2008). Here, we found 185 mRNAs or miRNA candidates to be cleaved by miRNAs in *M. truncatula* roots.

Identification of Novel miRNAs in *M. truncatula* Roots

By small RNA sequencing, we could detect 162 miRNAs expressed in *M. truncatula* roots, which are currently annotated at the miRBase database version 16. In addition to these known miRNAs, deep sequencing coupled with miRDeep predictions revealed 515 novel miRNA candidates of *M. truncatula* of 20 to 25 nucleotides. Although the majority of plant miRNAs reported so far are of 20 to 23 nucleotides in length, there are reports of 24-nucleotide miRNAs, like ath-miR163 (Park et al., 2002). In addition, ath-miR156, ath-miR395, ath-miR399, and other miRNAs can occur also as 23- to 25-nucleotide variants (Vazquez et al., 2008) and are then called long miRNAs. Such long miRNAs are processed by DCL3 (Vazquez et al., 2008). Unfortunately, DCL *M. truncatula* mutants are so far not available to test the DCL3 dependence of our 24- to 25-nucleotide miRNA candidates. The 24- to 25-nucleotide-long miRNAs and miRNA candidates have a considerably lower conservation (22%) in contrast to the 20- to 23-nucleotide-long miRNAs (59%), supporting the assumption that these long miRNAs might be of younger evolutionary origin. This is in line with the assumption that such young miRNAs derive from small inverted repeat loci in the genome (Vazquez et al., 2008).

The criteria for the annotation of novel miRNAs from high-throughput sequencing data have been reevaluated recently, since reanalysis of miRNA data sets of invertebrates and plants demonstrated a considerably high fraction of erroneously annotated miRNAs (Rajagopalan et al., 2006, Ruby et al., 2006, 2007). With the availability of deep sequencing, data are now possible and essential to confidently determine the precise 5′ end of a mature miRNA (Chiang et al., 2010; Berezikov et al., 2011). In addition, reads matching the miRNA* should be present and have the potential to pair to the mature miRNA candidate with approximately two-nucleotide 3′ overhangs (Chiang et al., 2010). Taking these two latter criteria into account, we identified 243 novel miRNAs of *M. truncatula*, which are now deposited at miRBase.

Distinct miRNAs Are Up-Regulated in Mycorrhizal Roots

The read count analysis of our miRNA candidates showed that members of 20 miRNAs are regulated in mycorrhizal roots as compared with nonmycorrhizal roots. For eight miRNAs of the most strongly regulated candidates ($\log_2$ fold > 1), a significant differential expression was proven by RT-PCR analysis. The highest

Table IV. *miRNA targets with differential transcript accumulation in mycorrhizal roots as compared with nonmycorrhizal roots*

Listed accession numbers of the mt3.0 and MtGI databases are nonredundant.

Target Identifier	Target Gene Family	LFC[a] (miRNA Target)	Cleavage Site	miRNA Identifier	Alignment Score	Category nm	Category myc	LFC[a] (miRNA)
Medtr8g109760.1	GRAS transcription factor	19.0	765	miR5204*	1.5	No tag	2	2.6
Medtr5g076920.1	Major facilitator superfamily	18.7	256	miR399a–q	5	No tag	0	−0.2 to +0.3
Medtr5g076920.1	Major facilitator superfamily	18.7	256	miR399r	4	No tag	0	0.2
Medtr7g102930.1	Blue copper binding	8.6	496	miR169d*/e.2*/l*/m*	5.5	No tag	3	4
Medtr5g084780.1	Glutathione *S*-transferase	8.6	892	miR5282	5.5	No tag	3	0
TC139113	EGF domain containing	5.6	72	miR5204*	2.5	No tag	4	2.6
Medtr3g150590.1	Heat shock DnaJ	3.2	1,684	miR166a–h	5.5	No tag	1	−0.1 to +0.3
TC138105	Kinase family	2.6	665	miR399q*	6	1	4	−0.6
AW687825	Glycogenin-like	2.3	463	miR5253	2.5	No tag	4	0.5
Medtr7g014850.1	MADS box transcription factor	2.1	977	miR164a–d	6	1	No tag	−1.5 to −0.7
AW697209	Hypothetical	1.9	161	miR5206	7	No tag	0	4.9
TC134204	TIR; resistance	1.8	187	miR5213	5	1	0	0.7
TC132098	Glycogenin-like	1.8	283	miR5253	2.5	No tag	4	0.5
TC125161	Hypothetical	1.8	47	miR164a/b/c	5.5	No tag	1	−0.7
Medtr6g015300.1	Biotin-binding site	1.7	531	miR2086	3	No tag	4	0.8
TC120550	Albumin I	1.7	349	miR2643	7	2	2	0.3
TC120550	Albumin I	1.7	511	miR172b	2.5	No tag	4	0.7
AW693165	TIR; disease resistance	1.7	122	miR399k*	6	No tag	1	−0.6
BQ138232	Hypothetical	1.7	170	miR1509b	5.5	4	0	2
Medtr3g097800.1	Nsp2, GRAS transcription factor	1.6	427	miR171h	3	0	0	1.1
Medtr4g018250.1	Hypothetical	1.5	172	miR399a/c/e/f/g/h/i/l/p	1.5	No tag	4	−0.2 to +0.2
Medtr4g018250.1	Hypothetical	1.5	172	miR399r	3.5	No tag	4	0.2
Medtr4g018250.1	Hypothetical	1.5	467	miR399b/d/j/k/m/n/o/q	4	No tag	0	−0.2 to +0.3
Medtr6g028360.1	TIR; disease resistance	−1.5	429	miR5213	4	2	0	0.7
Medtr3g103970.1	Squamosa promoter binding	−1.5	1,083	miR399b/d/j/k/m/n/o/q	1	No tag	0	0 to +0.7
Medtr3g103970.1	Squamosa promoter binding	−1.5	1,083	miR156j	2	No tag	0	−0.2
Medtr6g099150.1	TIR; elongation factor Ts	−1.5	699	miR1510a*	4	3	No tag	−0.6
Medtr2g046350.1	TIR; disease resistance	−1.6	140	miR1510a*	0.5	4	No tag	0
Medtr2g046350.1	TIR; disease resistance	−1.6	131	miR5213	5.5	3	2	0.7
Medtr7g121710.1	Auxin response factor	−1.6	1,406	miR160a–e	1.5	1	1	−0.3 to +2.4
Medtr7g121710.1	Auxin response factor	−1.6	1,406	miR160f	1	1	1	4.8
Medtr7g026570.1	Kinase	−1.7	196	miR399h*	5.5	0	No tag	0.4
TC123814	GRF transcription factor	−1.8	573	miR399h*	4	0	0	0 to +0.3
Medtr7g121610.1	Auxin response factor	−1.8	1,406	miR160a–e	1.5	1	1	−0.3 to +2.4
Medtr7g121610.1	Auxin response factor	−1.8	1,406	miR160f	1	1	1	4.1
TC127408	Auxin response factor	−1.8	1,407	miR160f	3.5	No tag	5	4.1
Medtr6g098880.1	TIR; disease resistance	−1.8	203	miR2678	0	4	No tag	0
Medtr6g098880.1	TIR; disease resistance	−1.8	194	miR5213	4	No tag	2	0.7
TC116942	TIR; disease resistance	−1.9	84	miR5213	4	0	No tag	0.7
TC129665	TIR; disease resistance	−1.9	927	miR1507	5.5	1	No tag	0.4
Medtr6g098900.1	TIR; disease resistance	−1.9	727	miR1510a*	4	3	No tag	−0.6
Medtr6g098900.1	TIR; disease resistance	−1.9	139	miR2678	2	4	No tag	0
Medtr4g114680.1	TIR; disease resistance	−2.0	678	miR1510a*	4	3	No tag	−0.6
Medtr4g114680.1	TIR; disease resistance	−2.0	153	miR2678	0.5	2	No tag	0
Medtr6g099020.1	TIR; disease resistance	−2.0	8,901	miR1510a*	4	3	No tag	−0.6
Medtr6g099090.1	TIR; disease resistance	−2.0	8,902	miR1510a*	4	3	No tag	−0.6
Medtr6g099090.1	TIR; disease resistance	−2.0	8,305	miR5213	4	0	No tag	0.7
TC138295	TIR; disease resistance	−2.0	132	miR5213	5	3	3	0.7
Medtr3g125280.3	Alcohol dehydrogenase superfamily	−2.1	424	miR172b,c	5	3	4	−0.1
Medtr6g099070.1	TIR; disease resistance	−2.1	741	miR1510a*	4	3	No tag	−0.6
Medtr6g099070.1	TIR; disease resistance	−2.1	153	miR2678	0.5	2	No tag	0
Medtr3g125230.2	Alcohol dehydrogenase superfamily	−2.2	222	miR2119	3.5	2	2	0.9
Medtr3g166270.1	Hypothetical	−2.3	55	miR2118	4.5	1	1	−0.4
Medtr4g069410.1	Male sterility	−2.3	347	miR5269b	2	4	No tag	0.4
Medtr4g133300.1	Hypothetical	−2.5	216	miR399a/c/e/f/g/h/i	1	4	No tag	−0.2 to +0.2

(*Table continues on following page.*)

Table IV. (*Continued from previous page.*)

Target Identifier	Target Gene Family	LFC[a] (miRNA Target)	Cleavage Site	miRNA Identifier	Alignment Score	Category nm	Category myc	LFC[a] (miRNA)
Medtr4g135410.1	Hypothetical	−2.5	89/216	miR399a/c/e/f/g/h/i/k/l/p	2/1	4	No tag	−0.2 to +0.2
Medtr4g135140.1	Hypothetical	−2.5	356	miR399c*/k*	2	4	No tag	−0.6 to -0.3
Medtr4g135420.1	Hypothetical	−2.8	134	miR399c*/k*	2	4	No tag	−0.6 to -0.3
BE999763	Senescence associated	−3.3	351/474	miR5211	5	4	4	0.5

[a]LFC, $\log_2$ fold change ($P \leq 0.05$; χ^2 test together with Benjamini-Hochberg P value correction).

up-regulation was observed for miR5229a/b ($\log_2$ fold of 9.7), which is remarkably high taking into account that cellular differences in miRNA expression are hardly detectable, since whole root samples were used for library construction. We found miR5229a/b exclusively expressed in mycorrhizal roots and highly abundant in arbuscule-containing cells, suggesting a specific role during arbuscule development. So far, no target for this novel miRNA could be detected, but in silico predictions suggest a transcript encoding a heme peroxidase to be a target of this miRNA. Heme peroxidases have multiple tissue-specific functions, such as removal of hydrogen peroxide, oxidation of toxic compounds, cell wall biosynthesis, defense responses, and auxin and ethylene metabolism (Welinder et al., 1992). Hydrogen peroxide accumulates in mycorrhizal roots preferentially in degenerating arbuscules (Salzer et al., 1999). Thus, it might be anticipated that the induction of miR5229a/b suppresses the heme peroxidase, leading to locally increased hydrogen peroxide accumulation in cells with degenerating arbuscules. Interestingly, a clear induction in mycorrhizal roots was also found for miR169d/l. miR169 targets the transcription factor *MtHAP2-1* and has been demonstrated to play an important role during nodule differentiation by restriction of *MtHAP2-1* expression to the nodule meristematic zone (Combier et al., 2006). The increased expression of this miRNA in mycorrhizal roots together with the accumulation in the phloem and around fungal hyphae give evidence that the miR169 family is also involved in the AM symbiosis. Moreover, miRNA* sequences of the miR169 family were also strongly induced in mycorrhizal roots and were shown to have a similar tissue-specific accumulation as mature miR169. Remarkably, we were able to identify *MtBcp1* to be a target of this miRNA*. *MtBcp1* encodes a protein specifically accumulating in the periarbuscular membrane (Pumplin and Harrison, 2009), and it might be speculated that the miR169* sequences accumulating in mycorrhizal roots are involved in restricting *MtBcp1* expression to arbuscule-containing cells. A further miRNA that was exclusively detectable in mycorrhizal roots was miR160f*, which was primarily detected in the phloem. However, the function of this miRNA* is yet elusive, because no targets were found by degradome sequencing. The same situation is true for miR5204. Nevertheless, several targets could be in silico predicted, including a heavy metal transport protein and a zinc finger transcription factor. Notably, miR5204 appears to be a phosphate-responsive miRNA and is located around individual arbuscules. We hypothesize that the presence of this miRNA correlates with the concentration of phosphate in distinct arbuscule-containing cells. Similar to miR160f*, the mycorrhiza-induced miR160c was predominantly localized in the phloem and targeted several transcripts of the auxin response factor gene family. Moreover, different transcripts of auxin response factors are additionally targeted by miRNA167. Targets for both miRNAs were confirmed independently by our degradome analysis and by Jagadeeswaran et al. (2009). Auxin has been demonstrated to play a crucial role in AM symbiosis, probably in the presymbiotic phase of AM fungal development (Hanlon and Coenen, 2011), and the auxin content is elevated in mycorrhizal roots (Fitze et al., 2005; Jentschel et al., 2007). The fact that both miRNAs were significantly up-regulated in mycorrhizal roots and target transcripts of the same gene family implies that miR160c and miR167 might be involved in the fine regulation of auxin responses in AM symbiosis. Future investigation will unravel the physiological relevance of the discussed miRNAs during AM symbiosis.

Regulation of Symbiosis-Relevant Transcripts by miRNAs

The transcriptome-wide degradome analysis applied here gives the unique opportunity to identify mRNAs that undergo miRNA-mediated cleavage. Besides *MtBcp1*, we identified further transcripts strongly induced in mycorrhizal roots to be miRNA targets (Table IV). *MtGst1*, encoding a mycorrhizal symbiosis-specific glutathione *S*-transferase (Wulf et al., 2003), is one example of a transcript being regulated by a pair of miRNAs (cleaved at different positions by miR5282 and the candidate miRNA new_miRc_275). This regulation by two miRNAs indicates that *MtGst1* levels need to be tightly controlled by the host plant to ensure a functional symbiosis. A similar phenomenon of a two-miRNA-mediated combinatorial regulation was previously described in *Vitis vinifera* (Pantaleo et al., 2010); here, both miR156 and miR535 each regulate three squamosa promoter-binding transcription factor genes. The analysis of the degradome data revealed at least eight additional differentially expressed transcripts being cleaved in a combinatorial mode of regulation (Table IV). A further symbiosis-relevant gene regulated

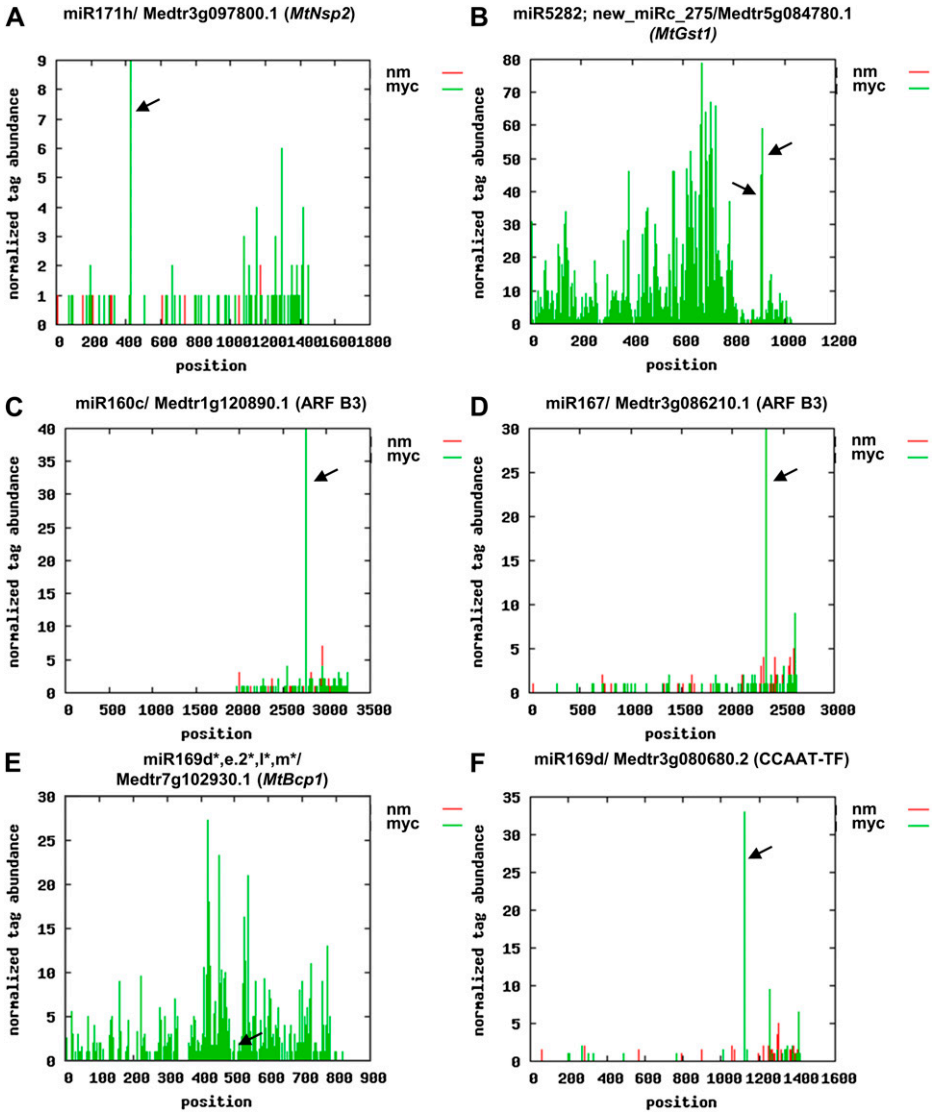

Figure 5. Target plots demonstrating miRNA-mediated transcript cleavage. Distribution of 5′ ends of the degradome tags within the full-length target mRNA sequence is shown. Tags aligned with cleavage sites of corresponding miRNAs are indicated by arrows. Target plots are shown for *MtNsp2* (A), *MtGst1* (B), auxin response factor (ARF) B3 (C), ARF B3 (D), *MtBcp1* (E), and CCAAT-binding transcription factor (F).

by a miRNA is *MtNsp2*, a GRAS transcription factor essential for root nodule development (Oldroyd and Long, 2003). In addition, *nsp2-2* mutants show decreased mycorrhizal colonization, which implies a role also during mycorrhizal signaling (Maillet et al., 2011). MtNSP2 forms a dimer with MtNSP1 to bind to the early-nodulin *MtEnod11* promoter (Hirsch et al., 2009). Surprisingly, we found significantly increased *MtNsp2* transcript levels in mycorrhizal roots, and *MtNsp2* transcripts are cleaved by miR171h. This implies that *MtNsp2* is both transcriptionally regulated and controlled by a miRNA. However, the role of these regulation steps in symbiosis signaling remains to be elucidated. Another GRAS transcription factor strongly induced in arbuscule-containing cells (N. Gaude, S. Bortfeld, N. Duensing, M. Lohse, and F. Krajinski, unpublished data) was found to be the most strongly up-regulated transcript comparing the read count within the degradome data of nonmycorrhizal versus mycorrhizal roots. Interestingly, this transcription factor is cleaved by miR5204*, whose corresponding mature strand itself is highly up-regulated in mycorrhizal roots (see above). This implies that the target is subjected to a strong spatial regulation by miR5204* in mycorrhizal roots. The second most up-regulated transcript encodes a major facilitator protein and is a new target for miR399, which is currently, besides PHO2 (Bari et al., 2006; Chiou et al., 2006), the second miR399 target identified. The strong transcriptional induction of this major facilitator gene and its regulation by miR399 further supports the role of miR399 during the cellular phosphate homeostasis regulation in mycorrhizal roots (Branscheid et al., 2010).

miRNA*-Mediated Target Cleavage

This study provides evidence for miRNA*-mediated mRNA cleavage in *M. truncatula* roots. Moreover, we often found a notably high accumulation of miRNA* and for several miRNA* molecules even a higher

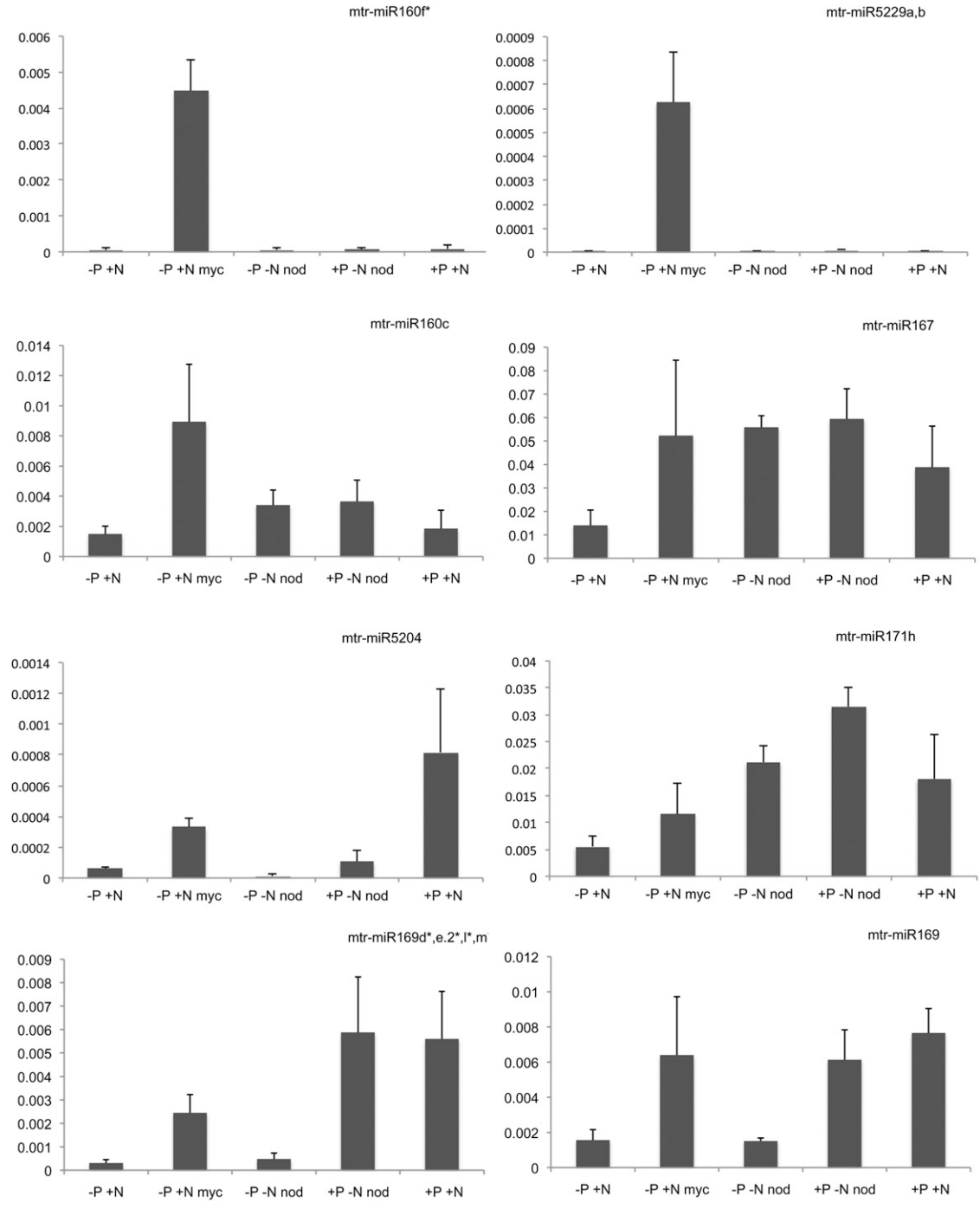

Figure 6. Relative abundance of AM symbiosis-induced mature miRNAs. The following conditions were applied, and roots were harvested 3 weeks after inoculation: −P, 20 μM phosphate fertilization; +P, 1 mM phosphate fertilization; −N, 0 μM nitrate; +N, 5 mM nitrate; myc, mycorrhizal roots; nod, nodulated by *S. meliloti*. If not indicated, roots were not inoculated with either of the two symbionts. Values shown are + SD of four biological replicates. Normalization was carried out against a reference gene index (*MtPdf2* or *MtEf1*). Primers were designed to measure specific miRNAs, if possible. If primers bind to more than one mature or star miRNA sequence, it is indicated here.

abundance as compared with their mature miRNAs. It is currently anticipated that one arm of the RNA duplex preferentially accumulates and is then referred to as mature miRNA, whereas the opposite strand is called miRNA*. Previous models suggested that the choice of the dominant miRNA arm encoding the mature miRNA depends on thermodynamic and structural properties of the duplex RNA molecule

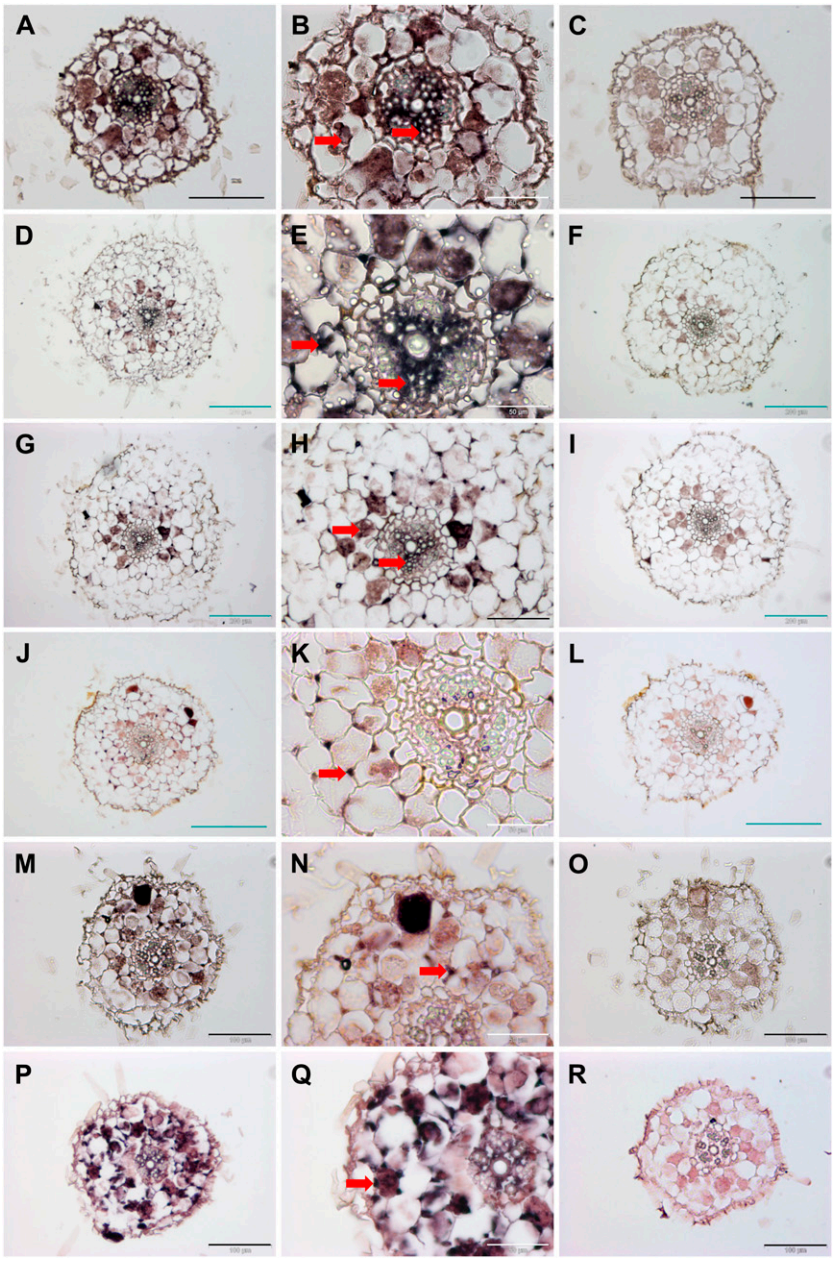

Figure 7. Tissue-specific expression of miRNAs in mycorrhizal roots. Cross-sections of mycorrhizal *M. truncatula* roots were hybridized to labeled locked nucleic acid probes complementary to selected miRNA or miRNA*. For each locked nucleic acid probe hybridization, adjacent sections were used for scramble probe hybridization. The following miRNA or miRNA* were analyzed: miR160c (A), with detail in B and scramble probe in C; miR160f (D), with detail in E and scramble probe in F; miR169 (G), with detail in H and scramble probe in I; miR169d*/l*/m*/e.2* (J), with detail in K and scramble probe in L; miR5204 (M), with detail in N and scramble probe in O; and miR5229a/b (P), with detail in Q and scramble probe in R. Red arrows represent examples of distinct signals indicating miRNA accumulation. White bars = 50 μm, black bars = 100 μm, and cyan bars = 200 μm.

(Khvorova et al., 2003, Schwarz et al., 2003). Nevertheless, it was recognized that many miRNA* species also accumulate to substantial levels and are able to down-regulate target mRNAs (Okamura et al., 2008; Yang et al., 2011). Moreover, large-scale sequencing data have shown that the arm from which the dominant form is processed can switch in different tissues (Chiang et al., 2010) and in different organisms (Griffiths-Jones et al., 2011). Interestingly, the in situ hybridizations confirmed the accumulation of miR169d*/e.2*/l*/m* and miR160f* in the intracellular space and phloem of the roots. Identical signal patterns were obtained for their corresponding mature strand or a mature strand of the same miRNA family, respectively. This is in line with previous findings from rapeseed (*Brassica napus*), where besides other miRNA*, considerable levels of miR169* and miR160* were detected in the phloem sap (Buhtz et al., 2008; Pant et al., 2009). Remarkably, we found for the star strands of miR160f, miR5204, miR169d*/e.2*/l*/m*, and miR396b* elevated levels in mycorrhizal roots (Table II). In tomato (*Solanum lycopersicum*), miR169g* was found to be up-regulated in leaves of mycorrhizal or high-phosphate-treated plants (Gu et al., 2010). The fact that both the mature miRNA and the corresponding miRNA* were present in the phloem might indicate that phloem-transported miRNAs, which act as long-distance signals (Pant et al., 2008), are transported as a miRNA/miRNA* duplex, probably due to a higher stability of such a duplex molecule. However, double-strand- or single-

strand-specific RNA nuclease assays did not prove the presence of RNA duplexes in the rapeseed phloem (Buhtz et al., 2008). However, it has been suggested that such duplex molecules are denatured during RNA extraction and therefore difficult to detect (Buhtz et al., 2008).

In addition to the previously discussed miRNAs, also the highly conserved mature miR399 was proven to be phloem transported from shoot to root (Pant et al., 2008), which is also true for miR399* (Hsieh et al., 2009). Our analysis revealed several targets for the star strands of miR399c,d,h,k,q (Table III). The detailed analysis of the miR399c*,k* targets (Medtr4g135140 and Medtr4g135420) revealed these genes to be duplicated genomic loci for primary transcripts of miR399j and miR399k. Both primary transcripts are inversely oriented and have a short overlap at the end of the putative transcript. Interestingly, this overlap appears to be the cleavage site for miR399c*,k*, which might be a mechanism of self-regulation of the miR399 genes. Cleavage of primary miRNA transcripts has been already observed in Arabidopsis and rice (German et al., 2008; Zhou et al., 2010b); therefore, self-regulation through a feedback circuit between primary miRNA transcripts and corresponding miRNA/miRNA* has been postulated (Meng et al., 2010). It was proposed that the overproduction of miRNA precursors results in an accumulation of miRNAs or miRNA*, which in turn could recognize their host precursors as the downstream targets. In contrast to this assumption, we found self-regulation for miRNAs with an even low abundance of overall reads. Expression of both strands showed the same level, indicating that the ratio between the mature and star strands might be involved in the self-regulation. The regulatory role of miRNA* sequences has also been observed in animals (Jagadeeswaran et al., 2010) and human, where miR-155* and miR-155 adjust their type I interferon production in an opposite manner through different targets (Zhou et al., 2010a). The degradome analysis applied here unraveled miRNA*-mediated mRNA cleavage of transcripts, which were distinct from transcripts targeted by the corresponding mature strand. One example is miR169, which targets a CCAAT transcription factor important for root nodule development (Combier et al., 2006), whereas the star strand, which is more abundant than the mature miR169 in mycorrhizal roots, mediates the cleavage of the arbuscule-specific protein MtBcp1. Hence, it might be anticipated that the dominant form of this miRNA switches during the two endosymbioses and restricts the expression of different targets to distinct cell types. In addition, we also found miRNAs for which targets were identified so far only for the miRNA*, particularly for miR5204*, which targets a GRAS transcription factor specifically expressed in mycorrhizal roots. In summary, our findings propose that the establishment of a mycorrhizal symbiosis leads to a reprogramming of the miRNA target network in roots, including miRNA strand preferences.

miRNAs Modulate the Defense Response upon Mycorrhizal Infection

Within the group of miRNA-mediated cleaved transcripts, transcription factors and disease resistance genes were clearly overrepresented. Most of the transcription factors are targeted by conserved miRNAs, which is in line with previous findings (Kidner and Martienssen, 2005). Our study indicates that four primarily moderately conserved miRNAs, namely miR1510a*, miR1507, miR2678 (Szittya et al., 2008; Lelandais-Brière et al., 2009), and miR5213, regulate disease resistance genes. Plants have evolved a general defense response to biotic interactions involving toll and interleukin-1 receptor (TIR)/nucleotide-binding site-Leu-rich repeat disease resistance genes and PR proteins (Jones and Dangl, 2006; Głowacki et al., 2011). Although basal defense mechanisms, which include the accumulation of phenolic compounds and PR proteins, are activated upon the interaction with AM fungi (Campos-Soriano et al., 2010; Abdel-Fattah et al., 2011), we observed that mRNA levels of many of the miRNA-targeted disease resistance genes are decreased in mycorrhizal roots. This might support the fungal growth within mycorrhizal roots. A similar phenomenon was described for a parasitic fungus-plant interaction; it is assumed that miRNA biogenesis and function is compromised in specific tissues in order to promote the activation of disease resistance genes to restrict the growth of biotrophic fungi (Lu et al., 2007). The degradome data demonstrate that a subset of defense response genes (Medtr6g098880.1, Medtr2g046350.1, and TC138295) is suppressed by miR5213 in mycorrhizal roots, and no specific miRNA cleavage was observed for these genes in nonmycorrhizal roots. Moreover, in nonmycorrhizal roots, the same subset of defense genes is regulated by miR2678, indicating a complex regulatory network of defense responses genes involving a combinatorial regulation by different miRNAs. Notably, miR5213, which mediated the cleavage of defense response transcripts, was conserved only in AM symbiosis-capable plants such as soybean, *L. japonicus*, and *P. trichocarpa* but not in Arabidopsis, which is not able to undergo this mutualistic association.

CONCLUSION

In summary, we were able to identify a high number of novel miRNAs in the roots of *M. truncatula*. Read count analysis together with qRT-PCR measurements and in situ hybridizations clearly indicated a regulation of miR5229a/b, miR5204, miR160f*, miR160c, miR169, and miR169d*/l*/m*/e.2* during AM symbiosis. Additionally, degradome sequencing provided evidence for the miRNA- and miRNA*-mediated regulation of several symbiosis-relevant genes and the repression of cellular defense responses in mycorrhizal roots. These findings provide a new basis for

investigating the regulatory network leading to cellular reprogramming during the interaction between plants and microsymbionts.

MATERIALS AND METHODS

Plant Material

Seeds of *Medicago truncatula* Jemalong A17 were germinated as described previously (Branscheid et al., 2010). Seedlings were grown in a sand:expanded clay substrate (1:1) under 16 h of light at 25°C and fertilized, unless otherwise noted, twice a week with half-strength Hoagland solution containing 20 μM phosphate. For inoculation with *Glomus intraradices*, an inoculum was added to the substrate at 10% (v/v). *G. intraradices* (strain BB-E; provided by Agrauxine) was propagated on *Allium porrum* plants, which were fertilized twice a week with half-strength Hoagland solution containing 20 μM phosphate. After 4 months, the *A. porrum* plants were harvested and the growth substrate was used as inoculum for *M. truncatula* seedlings. Plants were harvested 3 weeks after inoculation, representative parts of the roots were stained with WGA-Alexa Fluor 588 (Invitrogen) to estimate mycorrhizal colonization, and remaining roots were immediately frozen in liquid nitrogen or embedded in Paraplast. Mycorrhizal colonization was estimated as described (Trouvelot et al., 1986). Under the conditions described, *M. truncatula* roots were completely (frequency of mycorrhizal colonization in the root system = 100%) colonized by *G. intraradices*.

Inoculation with *Sinorhizobium meliloti*

For the inoculation of *M. truncatula* roots with *S. meliloti*, the bacteria were grown in 25 mL of tryptone yeast medium containing 4.5 mM $CaCl_2$ at 28°C to an optical density at 600 nm of about 0.5. Prior to inoculation, the culture was diluted 1:10 with water and seedlings were inoculated by watering. Control plants were mock inoculated with 1:10 diluted tryptone yeast medium. Plants were harvested 3 weeks after inoculation, and mature root nodules were visible.

Construction, Cloning, and Deep Sequencing of Small RNA Libraries

Total RNA was isolated using the mirVana miRNA isolation kit (Ambion) in combination with the Plant RNA Isolation Aid (Ambion). RNA at 10 μg was used for small RNA library construction using the Digital Gene Expression Small RNA Sample Prep Kit (Illumina). A quality control was carried out by TOPO TA cloning (Invitrogen) and Sanger sequencing of 100 clones. Illumina-Solexa sequencing was performed at FASTERIS.

Annotation Data

M. truncatula genomic, cDNA, bacterial artificial chromosome sequence, and annotation data for the releases mt1.0 to mt3.0 were downloaded from the *M. truncatula* project Web page (http://mips.helmholtz-muenchen.de/plant/medi3/index.jsp). rRNA and tRNA sequences were collected from the National Center for Biotechnology Information (http://www.ncbi.nlm.nih.gov), PlantGDB (http://www.plantgdb.org), and Rfam (Griffiths-Jones, 2009) databases. miRNA sequences (mature, star, and precursor) were downloaded from miRBase (version16; Griffiths-Jones et al., 2008). For miRNA genes, where no star sequence was annotated, we defined the star sequence according to known Dicer-cleavage rules as implemented in the miRDeep software tool (Friedländer et al., 2008). Transposable element sequence information was extracted from the GFF file provided by the *M. truncatula* genome project.

isomiRs and miRNA Sibling Data Processing for Known miRNAs

For annotating isomiRs (Vazquez et al., 2008) and miR siblings (Zhang et al., 2010), we used all reads from the small RNA libraries that could be mapped in the sense direction without any mismatch onto the in miRBase16 annotated miRNA precursor sequences having a minimum abundance of 20 reads, but not representing annotated miRNA mature and star sequences. We defined isomiRs as reads that are not shifted more than five positions from their original mature or star 5′ position. miRNA siblings were then all other reads that could be mapped to the miRNA precursor.

Small RNA Deep Sequencing and Sequence Processing

The small RNA reads were 3′ trimmed using the NOVOALIGN software (http://www.novocraft.com). The reads of both libraries were mapped to the *M. truncatula* genome, annotated cDNA sequences, and annotated noncoding RNA sequences using RazerS (Weese et al., 2009). Matching was done using 100% (no mismatch) as the identity threshold.

The small RNA data were normalized to "reads per million" per library by dividing the read number of each individual small RNA sequence by the number of redundant reads (15–31 nucleotides) in each library multiplied by 1 million. To investigate the read counts for known miRNAs (miRBase release 16; Griffiths-Jones et al., 2008) and to find statistically significant changes in read distributions, we used the χ^2 test together with Benjamini-Hochberg P value correction (false discovery rate of 0.05) as described previously by Pant et al. (2009).

miRNA Prediction

For the prediction of potential miRNAs, all reads matching with no mismatch to *M. truncatula* cDNA, annotated miRNA, tRNA, rRNA, or other noncoding RNA sequences were removed. For every condition, only reads with a minimum abundance of 20 reads having at most 25 distinct matches on the *M. truncatula* genome were used for further processing.

The original miRDeep software (Friedländer et al., 2008) was adjusted to take account of plant-specific miRNA features like longer precursor sequences, precursors having noncanonical hairpin structures, and more diverse read distributions of sequenced small RNAs. Therefore, a new tool was developed to excise candidate precursor regions using the mapped small RNA reads as input, RNAhybrid (Rehmsmeier et al., 2004) for searching up to five best hybridizations for a mapped small RNA within a maximal window size of 1,000 nucleotides upstream and downstream of the genomic mapping having a minimum hybridization energy (the threshold was derived for mature Arabidopsis [*Arabidopsis thaliana*] miRNAs from miRBase 14), and RNAfold (Gruber et al., 2008) from the Vienna package (version 1.8.2) to fold the candidate regions. The excised sequences were then filtered according to plant-specific precursor features for canonical and noncanonical hairpin structures derived from miRBase 14 for plant precursor, like minimum free energy, number of base pairs, number of nonpaired bases, and duplex length. The potential precursor sequences from both conditions were then clustered using the software cd-hit (Li and Godzik, 2006) demanding 100% sequence identity and a maximal sequence length difference per cluster of 30 nucleotides. From every cluster, the longest precursor sequence was chosen. In the next step, for each condition separately, all reads of length 15 to 31 nucleotides were mapped to the candidate precursor sequences using RazerS in the forward direction allowing no mismatch. The output was then transformed into the BLAST-parsed format used as input for the miRDeep core algorithm. The miRDeep core algorithm was adjusted based on the mapping of small RNA data from Pant et al. (2009) to miRBase 14 Arabidopsis precursor sequences allowing for noncanonical hairpin structures and more inconsistencies with the assumed Dicer processing. Predicted miRNAs were checked for overlaps with annotated miRNAs, noncoding RNAs, and protein-coding genes. As an additional filter for the miRDeep predicted miRNAs, we used two measures introduced for the miRTrap algorithm (Hendrix et al., 2010): the Hmax (for 5′ heterogeneity) and the AAPD (average antisense product displacement) parameters. Both parameters were adjusted for Arabidopsis using the miRBase version 14 annotations and the deep sequencing data from Pant et al. (2009). The miRDeep predictions are further classified into canonical and noncanonical hairpin structures and strict (original miRDeep core algorithm parameter) and nonstrict (allowing for more inconsistencies for the read distribution on the precursor).

Construction and Cloning of Degradome Libraries

An aliquot of the RNA sample used for small RNA sequencing was used for generating a degradome library. Poly(A) RNA was isolated from total RNA using the Oligotex mRNA Kit (Qiagen). The degradome libraries from 1 μg of poly(A)-enriched RNA were generated according to German et al. (2009). To perform a quality check prior to sequencing, an aliquot of the blunt-ended

cDNA was adenylated using dATP and GoTaq (Promega) for 10 min at 72°C and was cloned using the TOPO TA Cloning Kit (Invitrogen) for subsequent sequencing of 24 colonies per library. Illumina-Solexa sequencing of both degradome libraries was performed at FASTERIS.

Degradome Analysis

After sequencing the degradome library, sequence tags of 20 and 21 nucleotides long were used after trimming sequence adapters and low-complexity regions (see small RNA data processing). The 20- and 21-nucleotide reads of both degradome (myc and nm) libraries were subjected to the CleaveLand 2.0 pipeline for small RNA target identification as described previously (Addo-Quaye et al., 2009). Briefly, the distinct reads were normalized to give reads per million and subsequently mapped to annotated cDNA, untranslated region, intron, transposon, and 1-kb upstream and downstream sequences of the *M. truncatula* genome version 3.0 or to *M. truncatula* annotated cDNA sequences from the Gene Index database at the Dana-Farber Cancer Institute (MtGI release 9.0).

As small read input for the CleaveLand pipeline, we used either registered (miRBase release 16) or miRDeep-predicted miRNAs. We ran CleaveLand with default parameters using 100 randomized sequence shuffles. To clearly identify targets in the degradome libraries, CleaveLand categorizes all hits based on the abundance of the mRNA target tag relative to the overall abundance of degradome tags matching the target mRNA (Addo-Quaye et al., 2009).

qRT-PCR Analysis

Quantification of mature miRNAs by qRT-PCR was carried out as described (Pant et al., 2008) with a minor change. To the stem-loop RT reaction, we additionally added 1 μL (0.5 μg) of oligo(dT)$_{18}$ primer. The relative mature miRNA abundance was calculated relative to the expression of the reference genes *MtEf1α* and *MtPdf2*. All primer sequences are listed in Supplemental Table S8.

In Situ Hybridization with Digoxigenin-Labeled Locked Nucleic Acid Probes

Sections were deparaffinized (100% xylene, 50% xylene in ethanol, 100% ethanol, 50% ethanol in diethyl pyrocarbonate-water, diethyl pyrocarbonate-water; 5 min at each step), deproteinated (1 μg mL^{-1} proteinase K in Tris (hydroxymethyl)aminomethane-ethylenediaminetetraacetic acid buffer; 5 min at 37°C), and fixed in 4% paraformaldehyde (10 min at room temperature). To avoid the loss of miRNA molecules, an additional step for the irreversible immobilization of miRNAs was included. Fixation using 1-ethyl-3-(3-dimethylaminopropyl)carbodiimide was done as described (Pena et al., 2009). Afterward, the sections were acetylated (triethanol amine, concentrated HCl, acetic anhydride) and dehydrated by an ethanol series (25%, 50%, 70%, 85%, 90%, and 100%; 30 s at each step). The sections were dried at room temperature and subsequently hybridized in ENZO hybridization buffer (ENZO Life Sciences) containing 0.4 pmol μL^{-1} appropriate digoxigenin-labeled locked nucleic acid detection probe. The whole procedure of hybridization, stringency washes, and immunological detection using nitroblue tetrazolium/5-bromo-4-chloro-3-indolyl phosphate was carried out according to Nuovo (2010).

Sequence data can be found under National Center for Biotechnology Information Gene Expression Omnibus series number GSE26218.

Supplemental Data

The following materials are available in the online version of this article.

Supplemental Figure S1. Correlation of $\log_2$ fold changes myc versus nm obtained by degradome library sequencing and *Medicago* genome array hybridization (Gomez et al., 2009).

Supplemental Table S1. Known miRNAs from *M. truncatula* identified by homology and their most abundant isoforms.

Supplemental Table S2. New miRBase-deposited miRNAs from *M. truncatula*.

Supplemental Table S3. New miRDeep-predicted miRNA candidates from *M. truncatula*.

Supplemental Table S4. mt3.0 targets of known (miRBase 16) *M. truncatula* miRNAs identified by CleaveLand 2.0 (Addo-Quaye et al., 2009) and MtGI9 targets of known *M. truncatula* miRNAs (miRBase 15) using CleaveLand 2.0 (Addo-Quaye et al., 2009).

Supplemental Table S5. mt3.0 targets of novel miRBase-deposited *M. truncatula* miRNAs identified by CleaveLand 2.0 (Addo-Quaye et al., 2009) and MtGI9 targets of novel miRBase-deposited miRNAs identified by CleaveLand 2.0 (Addo-Quaye et al., 2009).

Supplemental Table S6. mt3.0 targets of miRDeep-predicted miRNA candidates of *M. truncatula* miRNAs identified by CleaveLand 2.0 (Addo-Quaye et al., 2009) and MtGI9 targets of miRDeep-predicted miRNA candidates identified by CleaveLand 2.0 (Addo-Quaye et al., 2009).

Supplemental Table S7. Accession numbers of targets listed in Table II.

Supplemental Table S8. Oligonucleotide sequences.

ACKNOWLEDGMENTS

We are grateful to Daniela Zoeller for help with plant growth and harvesting. We thank Samuel Griffith-Jones for help in annotating miRNAs, Przemyslaw Nuc for helpful discussions, and Marc Lohse for providing the updated *Medicago* MapMan annotation. We thank Manuel Spannagl for providing mt3.0 information and data. We thank the International Medicago Sequencing Consortium and the International Medicago Genome Annotation Group. The 3.0 data (IMGAG + additional Illumina sequences) are available at http://mips.helmholtz-muenchen.de/plant/medi3/index.jsp.

Received January 14, 2011; accepted May 6, 2011; published May 13, 2011.

LITERATURE CITED

Abdel-Fattah GM, El-Haddad SA, Hafez EE, Rashad YM (2011) Induction of defense responses in common bean plants by arbuscular mycorrhizal fungi. Microbiol Res **166:** 268–281

Addo-Quaye C, Eshoo TW, Bartel DP, Axtell MJ (2008) Endogenous siRNA and miRNA targets identified by sequencing of the Arabidopsis degradome. Curr Biol **18:** 758–762

Addo-Quaye C, Miller W, Axtell MJ (2009) CleaveLand: a pipeline for using degradome data to find cleaved small RNA targets. Bioinformatics **25:** 130–131

Akiyama K, Matsuzaki K, Hayashi H (2005) Plant sesquiterpenes induce hyphal branching in arbuscular mycorrhizal fungi. Nature **435:** 824–827

Bari R, Datt Pant B, Stitt M, Scheible WR (2006) PHO2, microRNA399, and PHR1 define a phosphate-signaling pathway in plants. Plant Physiol **141:** 988–999

Bartel DP (2004) MicroRNAs: genomics, biogenesis, mechanism, and function. Cell **116:** 281–297

Bartel DP (2009) MicroRNAs: target recognition and regulatory functions. Cell **136:** 215–233

Benedito VA, Li H, Dai X, Wandrey M, He J, Kaundal R, Torres-Jerez I, Gomez SK, Harrison MJ, Tang Y, et al (2010) Genomic inventory and transcriptional analysis of *Medicago truncatula* transporters. Plant Physiol **152:** 1716–1730

Berezikov E, Liu N, Flynt AS, Hodges E, Rooks M, Hannon GJ, Lai EC (2010) Evolutionary flux of canonical microRNAs and mirtrons in Drosophila. Nat Genet **42:** 6–9; author reply 9–10

Borsani O, Zhu J, Verslues PE, Sunkar R, Zhu JK (2005) Endogenous siRNAs derived from a pair of natural *cis*-antisense transcripts regulate salt tolerance in Arabidopsis. Cell **123:** 1279–1291

Boualem A, Laporte P, Jovanovic M, Laffont C, Plet J, Combier JP, Niebel A, Crespi M, Frugier F (2008) MicroRNA166 controls root and nodule development in *Medicago truncatula*. Plant J **54:** 876–887

Branscheid A, Sieh D, Pant BD, May P, Devers EA, Elkrog A, Schauser L, Scheible WR, Krajinski F (2010) Expression pattern suggests a role of MiR399 in the regulation of the cellular response to local Pi increase

during arbuscular mycorrhizal symbiosis. Mol Plant Microbe Interact **23:** 915–926

Brodersen P, Sakvarelidze-Achard L, Bruun-Rasmussen M, Dunoyer P, Yamamoto YY, Sieburth L, Voinnet O (2008) Widespread translational inhibition by plant miRNAs and siRNAs. Science **320:** 1185–1190

Buhtz A, Springer F, Chappell L, Baulcombe DC, Kehr J (2008) Identification and characterization of small RNAs from the phloem of *Brassica napus*. Plant J **53:** 739–749

Cai X, Hagedorn CH, Cullen BR (2004) Human microRNAs are processed from capped, polyadenylated transcripts that can also function as mRNAs. RNA **10:** 1957–1966

Campos-Soriano L, García-Garrido JM, San Segundo B (2010) Activation of basal defense mechanisms of rice plants by *Glomus intraradices* does not affect the arbuscular mycorrhizal symbiosis. New Phytol **188:** 597–614

Carthew RW, Sontheimer EJ (2009) Origins and mechanisms of miRNAs and siRNAs. Cell **136:** 642–655

Chen C, Ridzon DA, Broomer AJ, Zhou Z, Lee DH, Nguyen JT, Barbisin M, Xu NL, Mahuvakar VR, Andersen MR, et al (2005) Real-time quantification of microRNAs by stem-loop RT-PCR. Nucleic Acids Res **33:** e179

Chen X (2008) MicroRNA metabolism in plants. Curr Top Microbiol Immunol **320:** 117–136

Chiang HR, Schoenfeld LW, Ruby JG, Auyeung VC, Spies N, Baek D, Johnston WK, Russ C, Luo S, Babiarz JE, et al (2010) Mammalian microRNAs: experimental evaluation of novel and previously annotated genes. Genes Dev **24:** 992–1009

Chinnusamy V, Gong Z, Zhu JK (2008) Nuclear RNA export and its importance in abiotic stress responses of plants. Curr Top Microbiol Immunol **326:** 235–255

Chiou TJ, Aung K, Lin SI, Wu CC, Chiang SF, Su CL (2006) Regulation of phosphate homeostasis by microRNA in *Arabidopsis*. Plant Cell **18:** 412–421

Combier JP, Frugier F, de Billy F, Boualem A, El-Yahyaoui F, Moreau S, Vernié T, Ott T, Gamas P, Crespi M, et al (2006) MtHAP2-1 is a key transcriptional regulator of symbiotic nodule development regulated by microRNA169 in *Medicago truncatula*. Genes Dev **20:** 3084–3088

Dai X, Zhuang Z, Zhao PX (2011) Computational analysis of miRNA targets in plants: current status and challenges. Brief Bioinform **12:** 115–121

Dunoyer P, Himber C, Voinnet O (2006) Induction, suppression and requirement of RNA silencing pathways in virulent *Agrobacterium tumefaciens* infections. Nat Genet **38:** 258–263

Ebhardt HA, Fedynak A, Fahlman RP (2010) Naturally occurring variations in sequence length creates microRNA isoforms that differ in argonaute effector complex specificity. Silence **1:** 12

Elbashir SM, Lendeckel W, Tuschl T (2001a) RNA interference is mediated by 21- and 22-nucleotide RNAs. Genes Dev **15:** 188–200

Elbashir SM, Martinez J, Patkaniowska A, Lendeckel W, Tuschl T (2001b) Functional anatomy of siRNAs for mediating efficient RNAi in *Drosophila melanogaster* embryo lysate. EMBO J **20:** 6877–6888

Fahlgren N, Howell MD, Kasschau KD, Chapman EJ, Sullivan CM, Cumbie JS, Givan SA, Law TF, Grant SR, Dangl JL, et al (2007) High-throughput sequencing of Arabidopsis microRNAs: evidence for frequent birth and death of MIRNA genes. PLoS ONE **2:** e219

Fiorilli V, Catoni M, Miozzi L, Novero M, Accotto GP, Lanfranco L (2009) Global and cell-type gene expression profiles in tomato plants colonized by an arbuscular mycorrhizal fungus. New Phytol **184:** 975–987

Fitze D, Wiepning A, Kaldorf M, Ludwig-Müller J (2005) Auxins in the development of an arbuscular mycorrhizal symbiosis in maize. J Plant Physiol **162:** 1210–1219

Frenzel A, Manthey K, Perlick AM, Meyer F, Pühler A, Küster H, Krajinski F (2005) Combined transcriptome profiling reveals a novel family of arbuscular mycorrhizal-specific *Medicago truncatula* lectin genes. Mol Plant Microbe Interact **18:** 771–782

Friedländer MR, Chen W, Adamidi C, Maaskola J, Einspanier R, Knespel S, Rajewsky N (2008) Discovering microRNAs from deep sequencing data using miRDeep. Nat Biotechnol **26:** 407–415

German MA, Luo S, Schroth G, Meyers BC, Green PJ (2009) Construction of Parallel Analysis of RNA Ends (PARE) libraries for the study of cleaved miRNA targets and the RNA degradome. Nat Protoc **4:** 356–362

German MA, Pillay M, Jeong DH, Hetawal A, Luo S, Janardhanan P, Kannan V, Rymarquis LA, Nobuta K, German R, et al (2008) Global identification of microRNA-target RNA pairs by parallel analysis of RNA ends. Nat Biotechnol **26:** 941–946

Ghildiyal M, Zamore PD (2009) Small silencing RNAs: an expanding universe. Nat Rev Genet **10:** 94–108

Głowacki S, Macioszek VK, Kononowicz AK (2011) R proteins as fundamentals of plant innate immunity. Cell Mol Biol Lett **16:** 1–24

Gomez SK, Harrison MJ (2009) Laser microdissection and its application to analyze gene expression in arbuscular mycorrhizal symbiosis. Pest Manag Sci **65:** 504–511

Gomez SK, Javot H, Deewatthanawong P, Torres-Jerez I, Tang Y, Blancaflor EB, Udvardi MK, Harrison MJ (2009) *Medicago truncatula* and *Glomus intraradices* gene expression in cortical cells harboring arbuscules in the arbuscular mycorrhizal symbiosis. BMC Plant Biol **9:** 10

Gregory BD, O'Malley RC, Lister R, Urich MA, Tonti-Filippini J, Chen H, Millar AH, Ecker JR (2008) A link between RNA metabolism and silencing affecting Arabidopsis development. Dev Cell **14:** 854–866

Griffiths-Jones S (2009) The role of RNA molecules in cellular biology. Brief Funct Genomics Proteomics **8:** 405–406

Griffiths-Jones S, Hui JH, Marco A, Ronshaugen M (2011) MicroRNA evolution by arm switching. EMBO Rep **12:** 172–177

Griffiths-Jones S, Saini HK, van Dongen S, Enright AJ (2008) miRBase: tools for microRNA genomics. Nucleic Acids Res **36:** D154–D158

Gruber AR, Lorenz R, Bernhart SH, Neuböck R, Hofacker IL (2008) The Vienna RNA websuite. Nucleic Acids Res **36:** W70–W74

Gu M, Xu K, Chen AQ, Zhu YY, Tang GL, Xu GH (2010) Expression analysis suggests potential roles of microRNAs for phosphate and arbuscular mycorrhizal signaling in *Solanum lycopersicum*. Physiol Plant **138:** 226–237

Hanlon MT, Coenen C (2011) Genetic evidence for auxin involvement in arbuscular mycorrhiza initiation. New Phytol **189:** 701–709

He L, Hannon GJ (2004) MicroRNAs: small RNAs with a big role in gene regulation. Nat Rev Genet **5:** 522–531

Hendrix D, Levine M, Shi W (2010) miRTRAP, a computational method for the systematic identification of miRNAs from high throughput sequencing data. Genome Biol **11:** R39

Hirsch S, Kim J, Muñoz A, Heckmann AB, Downie JA, Oldroyd GE (2009) GRAS proteins form a DNA binding complex to induce gene expression during nodulation signaling in *Medicago truncatula*. Plant Cell **21:** 545–557

Hohnjec N, Vieweg MF, Pühler A, Becker A, Küster H (2005) Overlaps in the transcriptional profiles of *Medicago truncatula* roots inoculated with two different *Glomus* fungi provide insights into the genetic program activated during arbuscular mycorrhiza. Plant Physiol **137:** 1283–1301

Hsieh LC, Lin SI, Shih ACC, Chen JW, Lin WY, Tseng CY, Li WH, Chiou TJ (2009) Uncovering small RNA-mediated responses to phosphate deficiency in Arabidopsis by deep sequencing. Plant Physiol **151:** 2120–2132

Jagadeeswaran G, Zheng Y, Li YF, Shukla LI, Matts J, Hoyt P, Macmil SL, Wiley GB, Roe BA, Zhang W, et al (2009) Cloning and characterization of small RNAs from *Medicago truncatula* reveals four novel legume-specific microRNA families. New Phytol **184:** 85–98

Jagadeeswaran G, Zheng Y, Sumathipala N, Jiang HB, Arrese EL, Soulages JL, Zhang WX, Sunkar R (2010) Deep sequencing of small RNA libraries reveals dynamic regulation of conserved and novel microRNAs and microRNA-stars during silkworm development. BMC Genomics **11:** 52

Javot H, Penmetsa RV, Terzaghi N, Cook DR, Harrison MJ (2007) A *Medicago truncatula* phosphate transporter indispensable for the arbuscular mycorrhizal symbiosis. Proc Natl Acad Sci USA **104:** 1720–1725

Jentschel K, Thiel D, Rehn F, Ludwig-Muller J (2007) Arbuscular mycorrhiza enhances auxin levels and alters auxin biosynthesis in *Tropaeolum majus* during early stages of colonization. Physiol Plant **129:** 320–333

Jones JD, Dangl JL (2006) The plant immune system. Nature **444:** 323–329

Jones-Rhoades MW, Bartel DP (2004) Computational identification of plant microRNAs and their targets, including a stress-induced miRNA. Mol Cell **14:** 787–799

Kaló P, Gleason C, Edwards A, Marsh J, Mitra RM, Hirsch S, Jakab J, Sims S, Long SR, Rogers J, et al (2005) Nodulation signaling in legumes requires NSP2, a member of the GRAS family of transcriptional regulators. Science **308:** 1786–1789

Khvorova A, Reynolds A, Jayasena SD (2003) Functional siRNAs and miRNAs exhibit strand bias. Cell **115:** 209–216

Kidner CA, Martienssen RA (2005) The developmental role of microRNA in plants. Curr Opin Plant Biol **8:** 38–44

Kosuta S, Chabaud M, Lougnon G, Gough C, Dénarié J, Barker DG, Bécard G (2003) A diffusible factor from arbuscular mycorrhizal fungi induces symbiosis-specific MtENOD11 expression in roots of *Medicago truncatula*. Plant Physiol **131:** 952–962

Kosuta S, Hazledine S, Sun J, Miwa H, Morris RJ, Downie JA, Oldroyd GE (2008) Differential and chaotic calcium signatures in the symbiosis signaling pathway of legumes. Proc Natl Acad Sci USA **105:** 9823–9828

Krajinski F, Frenzel A (2007) Towards the elucidation of AM-specific transcription in *Medicago truncatula*. Phytochemistry **68:** 75–81

Laporte P, Merchan F, Amor BB, Wirth S, Crespi M (2007) Riboregulators in plant development. Biochem Soc Trans **35:** 1638–1642

Lee Y, Kim M, Han J, Yeom KH, Lee S, Baek SH, Kim VN (2004) MicroRNA genes are transcribed by RNA polymerase II. EMBO J **23:** 4051–4060

Lelandais-Brière C, Naya L, Sallet E, Calenge F, Frugier F, Hartmann C, Gouzy J, Crespi M (2009) Genome-wide *Medicago truncatula* small RNA analysis revealed novel microRNAs and isoforms differentially regulated in roots and nodules. Plant Cell **21:** 2780–2796

Li W, Godzik A (2006) cd-hit: a fast program for clustering and comparing large sets of protein or nucleotide sequences. Bioinformatics **22:** 1658–1659

Li YF, Zheng Y, Addo-Quaye C, Zhang L, Saini A, Jagadeeswaran G, Axtell MJ, Zhang W, Sunkar R (2010) Transcriptome-wide identification of microRNA targets in rice. Plant J **62:** 742–759

Liu J, Blaylock LA, Endre G, Cho J, Town CD, VandenBosch KA, Harrison MJ (2003) Transcript profiling coupled with spatial expression analyses reveals genes involved in distinct developmental stages of an arbuscular mycorrhizal symbiosis. Plant Cell **15:** 2106–2123

Liu J, Carmell MA, Rivas FV, Marsden CG, Thomson JM, Song JJ, Hammond SM, Joshua-Tor L, Hannon GJ (2004) Argonaute2 is the catalytic engine of mammalian RNAi. Science **305:** 1437–1441

Liu PP, Montgomery TA, Fahlgren N, Kasschau KD, Nonogaki H, Carrington JC (2007) Repression of AUXIN RESPONSE FACTOR10 by microRNA160 is critical for seed germination and post-germination stages. Plant J **52:** 133–146

Lu C, Jeong DH, Kulkarni K, Pillay M, Nobuta K, German R, Thatcher SR, Maher C, Zhang L, Ware D, et al (2008) Genome-wide analysis for discovery of rice microRNAs reveals natural antisense microRNAs (nat-miRNAs). Proc Natl Acad Sci USA **105:** 4951–4956

Lu S, Sun YH, Amerson H, Chiang VL (2007) MicroRNAs in loblolly pine (Pinus taeda L.) and their association with fusiform rust gall development. Plant J **51:** 1077–1098

Lu XY, Huang XL (2008) Plant miRNAs and abiotic stress responses. Biochem Biophys Res Commun **368:** 458–462

Maillet F, Poinsot V, André O, Puech-Pagès V, Haouy A, Gueunier M, Cromer L, Giraudet D, Formey D, Niebel A, et al (2011) Fungal lipochitooligosaccharide symbiotic signals in arbuscular mycorrhiza. Nature **469:** 58–63

Martinez J, Patkaniowska A, Urlaub H, Lührmann R, Tuschl T (2002) Single-stranded antisense siRNAs guide target RNA cleavage in RNAi. Cell **110:** 563–574

Meister G, Landthaler M, Patkaniowska A, Dorsett Y, Teng G, Tuschl T (2004) Human Argonaute2 mediates RNA cleavage targeted by miRNAs and siRNAs. Mol Cell **15:** 185–197

Meng Y, Gou L, Chen D, Wu P, Chen M (2010) High-throughput degradome sequencing can be used to gain insights into microRNA precursor metabolism. J Exp Bot **61:** 3833–3837

Meyers BC, Axtell MJ, Bartel B, Bartel DP, Baulcombe D, Bowman JL, Cao X, Carrington JC, Chen X, Green PJ, et al (2008) Criteria for annotation of plant microRNAs. Plant Cell **20:** 3186–3190

Navarro L, Dunoyer P, Jay F, Arnold B, Dharmasiri N, Estelle M, Voinnet O, Jones JD (2006) A plant miRNA contributes to antibacterial resistance by repressing auxin signaling. Science **312:** 436–439

Navarro L, Jay F, Nomura K, He SY, Voinnet O (2008) Suppression of the microRNA pathway by bacterial effector proteins. Science **321:** 964–967

Nogueira FT, Sarkar AK, Chitwood DH, Timmermans MC (2006) Organ polarity in plants is specified through the opposing activity of two distinct small regulatory RNAs. Cold Spring Harb Symp Quant Biol **71:** 157–164

Nuovo GJ (2010) In situ detection of microRNAs in paraffin embedded, formalin fixed tissues and the co-localization of their putative targets. Methods **52:** 307–315

Okamura K, Phillips MD, Tyler DM, Duan H, Chou YT, Lai EC (2008) The regulatory activity of microRNA* species has substantial influence on microRNA and 3′ UTR evolution. Nat Struct Mol Biol **15:** 354–363

Oldroyd GE, Long SR (2003) Identification and characterization of nodulation-signaling pathway 2, a gene of *Medicago truncatula* involved in Nod actor signaling. Plant Physiol **131:** 1027–1032

Pant BD, Buhtz A, Kehr J, Scheible WR (2008) MicroRNA399 is a long-distance signal for the regulation of plant phosphate homeostasis. Plant J **53:** 731–738

Pant BD, Musialak-Lange M, Nuc P, May P, Buhtz A, Kehr J, Walther D, Scheible WR (2009) Identification of nutrient-responsive Arabidopsis and rapeseed microRNAs by comprehensive real-time polymerase chain reaction profiling and small RNA sequencing. Plant Physiol **150:** 1541–1555

Pantaleo V, Saldarelli P, Miozzi L, Giampetruzzi A, Gisel A, Moxon S, Dalmay T, Bisztray G, Burgyan J (2010) Deep sequencing analysis of viral short RNAs from an infected Pinot Noir grapevine. Virology **408:** 49–56

Papp I, Mette MF, Aufsatz W, Daxinger L, Schauer SE, Ray A, van der Winden J, Matzke M, Matzke AJ (2003) Evidence for nuclear processing of plant micro RNA and short interfering RNA precursors. Plant Physiol **132:** 1382–1390

Parádi I, van Tuinen D, Morandi D, Ochatt S, Robert F, Jacas L, Dumas-Gaudot E (2010) Transcription of two blue copper-binding protein isogenes is highly correlated with arbuscular mycorrhizal development in *Medicago truncatula*. Mol Plant Microbe Interact **23:** 1175–1183

Park MY, Wu G, Gonzalez-Sulser A, Vaucheret H, Poethig RS (2005) Nuclear processing and export of microRNAs in Arabidopsis. Proc Natl Acad Sci USA **102:** 3691–3696

Park W, Li J, Song R, Messing J, Chen X (2002) CARPEL FACTORY, a Dicer homolog, and HEN1, a novel protein, act in microRNA metabolism in *Arabidopsis thaliana*. Curr Biol **12:** 1484–1495

Pena JT, Sohn-Lee C, Rouhanifard SH, Ludwig J, Hafner M, Mihailovic A, Lim C, Holoch D, Berninger P, Zavolan M, et al (2009) miRNA in situ hybridization in formaldehyde and EDC-fixed tissues. Nat Methods **6:** 139–141

Phillips JR, Dalmay T, Bartels D (2007) The role of small RNAs in abiotic stress. FEBS Lett **581:** 3592–3597

Pumplin N, Harrison MJ (2009) Live-cell imaging reveals periarbuscular membrane domains and organelle location in *Medicago truncatula* roots during arbuscular mycorrhizal symbiosis. Plant Physiol **151:** 809–819

Rajagopalan R, Vaucheret H, Trejo J, Bartel DP (2006) A diverse and evolutionarily fluid set of microRNAs in Arabidopsis thaliana. Genes Dev **20:** 3407–3425

Rehmsmeier M, Steffen P, Hochsmann M, Giegerich R (2004) Fast and effective prediction of microRNA/target duplexes. RNA **10:** 1507–1517

Rhoades MW, Reinhart BJ, Lim LP, Burge CB, Bartel B, Bartel DP (2002) Prediction of plant microRNA targets. Cell **110:** 513–520

Ruby JG, Jan C, Player C, Axtell MJ, Lee W, Nusbaum C, Ge H, Bartel DP (2006) Large-scale sequencing reveals 21U-RNAs and additional microRNAs and endogenous siRNAs in C. elegans. Cell **127:** 1193–1207

Ruby JG, Stark A, Johnston WK, Kellis M, Bartel DP, Lai EC (2007) Evolution, biogenesis, expression, and target predictions of a substantially expanded set of Drosophila microRNAs. Genome Res **17:** 1850–1864

Salzer P, Corbière H, Boller T (1999) Hydrogen peroxide accumulation in *Medicago truncatula* roots colonized by the arbuscular mycorrhiza-forming fungus *Glomus intraradices*. Planta **208:** 319–325

Schwarz DS, Hutvágner G, Du T, Xu Z, Aronin N, Zamore PD (2003) Asymmetry in the assembly of the RNAi enzyme complex. Cell **115:** 199–208

Subramanian S, Fu Y, Sunkar R, Barbazuk WB, Zhu JK, Yu O (2008) Novel and nodulation-regulated microRNAs in soybean roots. BMC Genomics **9:** 160

Sunkar R, Chinnusamy V, Zhu J, Zhu JK (2007) Small RNAs as big players in plant abiotic stress responses and nutrient deprivation. Trends Plant Sci **12:** 301–309

Szittya G, Moxon S, Santos DM, Jing R, Fevereiro MP, Moulton V, Dalmay T (2008) High-throughput sequencing of *Medicago truncatula* short RNAs identifies eight new miRNA families. BMC Genomics **9:** 593

Trouvelot A, Kough JL, Gianinazzi-Pearson V (1986) Mesure du taux de

mycorhization VA d'un système radiculaire. Recherche des méthodes d'estimation ayant une signification fonctionnelle. *In* V Gianinazzi-Pearson, S Gianinazzi, eds, The Mycorrhizae: Physiology and Genetic. INRA Press, Paris, pp 217–221

Usadel B, Nagel A, Thimm O, Redestig H, Blaesing OE, Palacios-Rojas N, Selbig J, Hannemann J, Piques MC, Steinhauser D, et al (2005) Extension of the visualization tool MapMan to allow statistical analysis of arrays, display of corresponding genes, and comparison with known responses. Plant Physiol **138:** 1195–1204

Vaucheret H, Vazquez F, Crété P, Bartel DP (2004) The action of ARGONAUTE1 in the miRNA pathway and its regulation by the miRNA pathway are crucial for plant development. Genes Dev **18:** 1187–1197

Vazquez F, Blevins T, Ailhas J, Boller T, Meins F Jr (2008) Evolution of Arabidopsis MIR genes generates novel microRNA classes. Nucleic Acids Res **36:** 6429–6438

Vazquez F, Gasciolli V, Crété P, Vaucheret H (2004) The nuclear dsRNA binding protein HYL1 is required for microRNA accumulation and plant development, but not posttranscriptional transgene silencing. Curr Biol **14:** 346–351

Voinnet O (2008) Post-transcriptional RNA silencing in plant-microbe interactions: a touch of robustness and versatility. Curr Opin Plant Biol **11:** 464–470

Voinnet O (2009) Origin, biogenesis, and activity of plant microRNAs. Cell **136:** 669–687

Wang Y, Juranek S, Li H, Sheng G, Tuschl T, Patel DJ (2008a) Structure of an argonaute silencing complex with a seed-containing guide DNA and target RNA duplex. Nature **456:** 921–926

Wang Y, Sheng G, Juranek S, Tuschl T, Patel DJ (2008b) Structure of the guide-strand-containing argonaute silencing complex. Nature **456:** 209–213

Weese D, Emde AK, Rausch T, Döring A, Reinert K (2009) RazerS: fast read mapping with sensitivity control. Genome Res **19:** 1646–1654

Welinder KG, Mauro JM, Nørskov-Lauritsen L (1992) Structure of plant and fungal peroxidases. Biochem Soc Trans **20:** 337–340

Willmann MR, Poethig RS (2007) Conservation and evolution of miRNA regulatory programs in plant development. Curr Opin Plant Biol **10:** 503–511

Wulf A, Manthey K, Doll J, Perlick AM, Linke B, Bekel T, Meyer F, Franken P, Küster H, Krajinski F (2003) Transcriptional changes in response to arbuscular mycorrhiza development in the model plant *Medicago truncatula*. Mol Plant Microbe Interact **16:** 306–314

Xie Z, Johansen LK, Gustafson AM, Kasschau KD, Lellis AD, Zilberman D, Jacobsen SE, Carrington JC (2004) Genetic and functional diversification of small RNA pathways in plants. PLoS Biol **2:** E104

Xie Z, Kasschau KD, Carrington JC (2003) Negative feedback regulation of Dicer-Like1 in Arabidopsis by microRNA-guided mRNA degradation. Curr Biol **13:** 784–789

Yang JS, Phillips MD, Betel D, Mu P, Ventura A, Siepel AC, Chen KC, Lai EC (2011) Widespread regulatory activity of vertebrate microRNA* species. RNA **17:** 312–326

Yang Z, Ebright YW, Yu B, Chen X (2006) HEN1 recognizes 21-24 nt small RNA duplexes and deposits a methyl group onto the 2′ OH of the 3′ terminal nucleotide. Nucleic Acids Res **34:** 667–675

Yu B, Yang Z, Li J, Minakhina S, Yang M, Padgett RW, Steward R, Chen X (2005) Methylation as a crucial step in plant microRNA biogenesis. Science **307:** 932–935

Zhang W, Gao S, Zhou X, Xia J, Chellappan P, Zhang X, Jin H (2010) Multiple distinct small RNAs originate from the same microRNA precursors. Genome Biol **11:** R81

Zhao B, Ge L, Liang R, Li W, Ruan K, Lin H, Jin Y (2009) Members of miR-169 family are induced by high salinity and transiently inhibit the NF-YA transcription factor. BMC Mol Biol **10:** 29

Zhou H, Huang X, Cui H, Luo X, Tang Y, Chen S, Wu L, Shen N (2010a) miR-155 and its star-form partner miR-155* cooperatively regulate type I interferon production by human plasmacytoid dendritic cells. Blood **116:** 5885–5894

Zhou M, Gu L, Li P, Song X, Wei L, Chen Z, Cao X (2010b) Degradome sequencing reveals endogenous small RNA targets in rice (*Oryza sativa* L. ssp. *indica*). Front Biol **1:** 67–90

Zhou X, Wang G, Zhang W (2007) UV-B responsive microRNA genes in *Arabidopsis thaliana*. Mol Syst Biol **3:** 103